ESPOO 2003 VTT PUBLICATIONS 499

Terho Kololuoma

Preparation of multifunctional coating materials and their applications

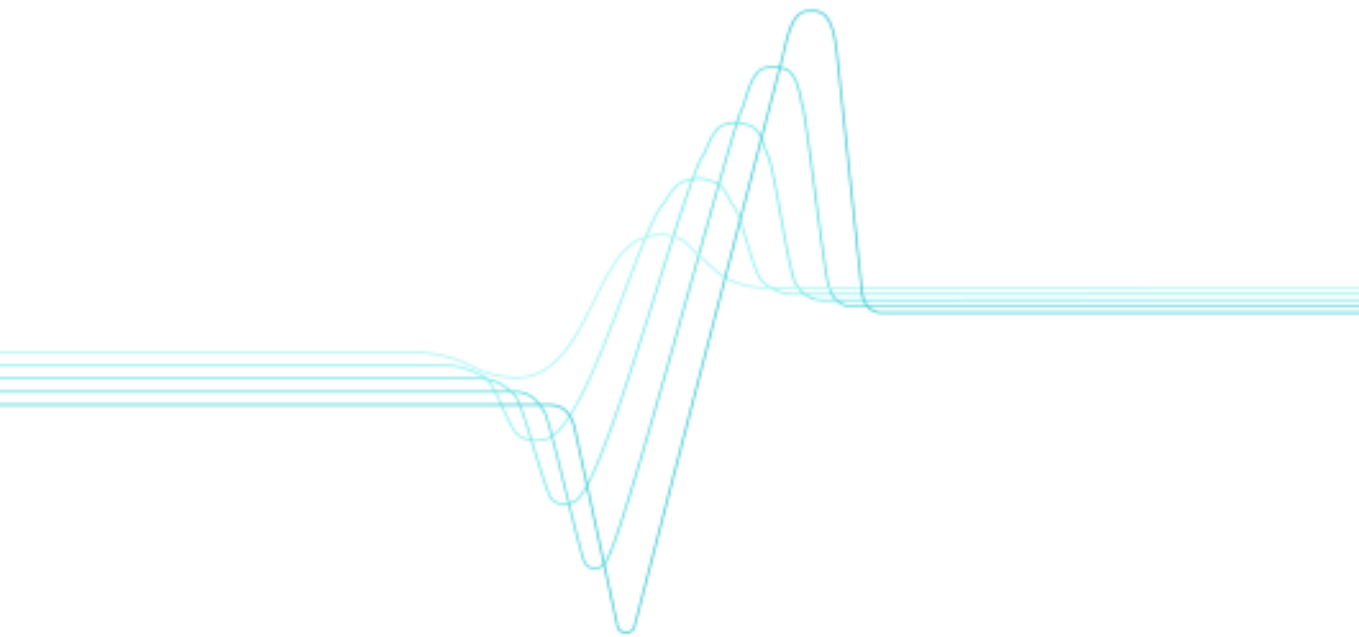

VTT PUBLICATIONS 499

Preparation of multifunctional coating materials and their applications

Terho Kololuoma

VTT Electronics

Academic Dissertation to be presented with the assent of Faculty of Science, University of Oulu, for public discussion in the Auditorium L10, Linnanmaa, on September 5th, 2003, at 12 o'clock noon.

ISBN 951–38–6227–5 (soft back ed.)
ISSN 1235–0621 (soft back ed.)

ISBN 951–38–6228–3 (URL: http://www.vtt.fi/inf/pdf/)
ISSN 1455–0849 (URL: http://www.vtt.fi/inf/pdf/)

JULKAISIJA – UTGIVARE – PUBLISHER

VTT, Vuorimiehentie 5, PL 2000, 02044 VTT
puh. vaihde (09) 4561, faksi (09) 456 4374

VTT, Bergsmansvägen 5, PB 2000, 02044 VTT
tel. växel (09) 4561, fax (09) 456 4374

VTT Technical Research Centre of Finland, Vuorimiehentie 5, P.O.Box 2000, FIN–02044 VTT, Finland
phone internat. + 358 9 4561, fax + 358 9 456 4374

VTT Elektroniikka, Kaitoväylä 1, PL 1100, 90571 OULU
puh. vaihde (08) 551 2111, faksi (08) 551 2320

VTT Elektronik, Kaitoväylä 1, PB 1100, 90571 ULEÅBORG
tel. växel (08) 551 2111, fax (08) 551 2320

VTT Electronics, Kaitoväylä 1, P.O.Box 1100, FIN–90571 OULU, Finland
phone internat. + 358 8 551 2111, fax + 358 8 551 2320

Technical editing Leena Ukskoski

Otamedia Oy, Espoo 2003

Kololuoma, Terho. Preparation of multifunctional coating materials and their applications. Espoo 2003, Technical Research Centre of Finland, VTT Publications 499. 62 p.+ app. 33 p.

Keywords sol-gel materials, antimony-doped tin dioxide, micro-optical elements, protective coatings

Abstract

Sol-gel technique has been utilized for the fabrication of multifunctional inorganic-organic hybrid materials for specific applications. Synthesized methacrylic acid and benzoylacetone modified tin alkoxide precursors were used for the first time for the realization of directly UV-photopatternable antimony-doped tin dioxide coatings. These single-layered coatings have transmission values over 80 % at visible wavelengths and maximum electrical conductivity values around 15 S/cm. In comparison, multi-layered coatings without UV-photopatternability properties were fabricated. In this case, electrical conductivities are in the range of 10^2 S/cm. A novel material technique approach for laser protective eyewear was utilized for the synthesis and preparation of the mechanically tolerant and near-infrared absorbing filter coatings. Optical densities from 2 to 4 at laser threat wavelength, a ten fold increase in scratch resistance, and a hundred-fold increase in abrasion resistance, compared to uncoated polycarbonate substrates, were obtained by using absorbing dye-molecule doped sol-gel materials. Fabrication of a diffractive optical element, namely axicon, using hybrid-glass materials was demonstrated for the first time. Hybrid-glass material was tailored to fulfill the requirements of the functional axicon element.

Preface

The present work was carried out at the Technical Research Centre of Finland, VTT Electronics, during the years 1999–2002.

My greatest thanks go to Docent J. Rantala who introduced me the fascinating world of sol-gel materials and for his continuous guidance, support and advice throughout the research. I also owe my gratitude to my supervisors Professor R. Laitinen, Department of Chemistry at the University of Oulu, and Professor H. Kopola, VTT Electronics, who encouraged and helped me in the course of this thesis.

I wish to thank Dr. P. Karioja for all the supporting projects, in which the research work for this thesis was possible to carry out. Also the Scientific Advisory Board for Defence (MATINE) and Graduate School of Electronics Manufacturing (Professor J. Kivilahti) are also greatly acknowledged for their financial support for the research work done during the research.

Many thanks go to my co-authors Dr. L.-S. Johansson, Dr. J. Campbell, Dr. J. Oksanen, Dr. P. Raerinne, Mr. A. Tolonen, Mrs. M. Tenhunen, Mr. T. Haatainen, Mr. K. Kataja, Mrs. S. Aikio and Mr. J. Aikio for their contributions. I thank all the staff in the VTT Electronics for the support they gave me. Especially, I wish to thank Dr. A. Maaninen, Mr. M. Keränen, Mr. J. Hiltunen, Mr. M. Tuomikoski and Ms. M. Kusevic for their friendship and support during this study.

Finally, I wish to thank my closest friends Tuukka and Iiku, Olli and Maja, and Pekka and Kimmo. I am extremely grateful to my bride-to-be, Jenni, who has helped me through all the hard moments. I also acknowledge the support I have received from my family.

The financial support provided by the Tauno Tönning Foundation is greatly acknowledged.

Oulu, June 2003

Terho Kololuoma

List of original publications

The present thesis consists of the following six papers, which will be referred to in the text by their Roman numerals (I–VI).

I Kololuoma, T. and Rantala, J. T. Effect of argon plasma treatment on the conductivity of sol-gel fabricated Sb doped SnO_2 thin films. Electronic Letters, 2000. Vol. 36, Issue 2, pp. 172–173.

II Kololuoma, T., Kärkkäinen, A. H. O. and Rantala, J. T. Novel synthesis route to conductive antimony doped tin dioxide and micro-fabrication method. Thin Solid Films, 2002. Vol. 408, pp. 128–131.

III Kololuoma, T., Johansson, L.-S., Campbell, J. M., Tolonen, A., Halttunen, M., Haatainen, T. and Rantala, J. T. The effect of UV-irradiation on antimony-doped tin dioxide thin films derived from methacrylic acid modified precursors. Chemistry of Materials, 2002. Vol. 14, pp. 4443–4447.

IV Kololuoma, T., Kärkkäinen, A. H. O., Tolonen, A. and Rantala, J. T. Lithographic patterning of benzoylacetone modified SnO_2 and Sb:SnO_2 thin films. Thin Solid Films, 2003. Accepted for publication.

V Kololuoma, T., Oksanen, J. A. I, Raerinne, P. and Rantala, J. T. Dye-doped sol-gel coatings for near-infrared laser protection. Journal of Materials Research, 2001. Vol. 16, pp. 2186–2188.

VI Kololuoma, T., Kataja, K., Juuso, S., Aikio, J. and Rantala, J. T. Fabrication and characterization of hybrid-glass-based axicons. Optical Engineering, 2002. Vol. 41, pp. 3136–3140.

The author of this thesis was the main author of all papers. In all papers the author developed and tailored the used multifunctional materials and also had a key role in the electrical and optical characterization, environmental stability testing and analysis of the results obtained during chemical characterization. In papers II–IV he was responsible for the idea of using organically modified alkoxide materials for the fabrication of directly UV-photopatternable antimony-doped organo-tin compounds. During the work in paper V, he resolved the problems related to the combination of absorbing dye molecules and a mechanically tolerant hybrid network. For paper VI, the author played a key role during the fabrication of the functional axicon elements with the help of the sol-gel derived hybrid-glass material.

Contents

Appendices of this publication are not included in the PDF version. Please order the printed version to get the complete publication (http://www.vtt.fi/inf/pdf/)

1. Introduction

The sol-gel technique is a synthetic route to solid and semi-solid materials via liquid phase processing. During the liquid phase processing, reactions between water and typically metal alkoxide precursors produce particulate or polymeric oxide materials. Because the by-products, typically water and alcohol, can be easily removed under thermal treatment of the oxide material, the final products have high purity. Liquid phase processing enables the molecular scale mixing of precursors, leading to homogeneous, multi-component materials. Moreover, through the precise control of processing parameters, various material shapes including powders, fibers, monoliths and thin films can be achieved. From those, thin films for optics and optoelectronics applications have been attracting most of the interest due to the ease of coating fabrication using conventional dip-, spin- and spray-coating techniques and furthermore, the optical transparency of oxide materials.

From the advanced material point of view, the most interesting feature of sol-gel processing is its capability to synthesize a new type of materials called inorganic-organic hybrids. Hybrid materials have been realized by incorporating organic functionalities and inorganic material network via doping, e.g. organic dye-molecules in an inorganic matrix, or via covalent bonding of organic groups and inorganic backbone, e.g. organometallics. In general, it is complicated to fabricate these types of materials with other techniques.

There is a growing need for multi-functional optical materials in the field of optoelectrical module integration and miniaturization. In such modules, new types of electrical, optical, and optoelectrical materials and new fabrication methods for functional components are required. For future optical and optoelectronic components such as organic light emitting devices, optical filters and devices capable of modulating light, these multi-functional materials, which have inorganic and organic material properties, offer an extraordinary tool for the fabrication of easily processable, application-specific materials.

1.1 Scope of the present work

The purpose of this thesis is to summarize the material chemistry research work based on the use of multifunctional hybrid material coatings in optics and optoelectronics applications. The research work was carried out at VTT Electronics in close collaboration with Finnish industry and it is divided into three application areas: *(i)* transparent electric conductors, namely antimony-doped tin dioxides, *(ii)* mechanically tolerant laser protective eyewear, and *(iii*) materials for micro-optical applications.

For the cost-effective fabrication of conductive and transparent coatings using inexpensive precursors and simple processing techniques, a method of producing sol-gel derived antimony-doped tin dioxide thin films is presented in paper I. Paper I also introduces an argon-plasma effect on the conductivity values of these coatings.

Applications in which transparent conductors are used typically require the fine patterning of the conductive films. Conventional lithographic patterning of chemically durable oxide films involves the use of additional photoresist layers and harsh etching chemicals. Therefore, the main objective of this thesis was to investigate the possibilities to fabricate directly UV-photopatternable antimony-doped tin organo thin films using synthesized photoreactive tin alkoxide derivatives, which can be converted after patterning to crystalline oxides. Two different methods to obtain a simpler and more environmentally friendly patterning process are described in papers II and IV. In paper III, the unexpected effects of the UV-irradiation on the electrical properties of the final material, as shown in paper II, are analyzed.

The second field of application was laser protective eyewear for military applications. The aim of this research was to develop scratch and abrasion resistant coating material for polycarbonate visors which also had angle independent absorption properties at neodium doped yttrium-aluminum garnet laser (*Nd:YAG*) wavelength (1064 nm). The specified optical density goal is at least 4 at the specific laser-threat wavelength. Meanwhile, the coating has to possess high optical transparency (80 %) at visible wavelengths without disturbing the color vision. Paper V reports on the synthesis and characteristics of the mass production capable protective coating material.

For the micro-optical component demonstrator, a specialized diffractive optical element, namely axicons, was designed for the triangular measurement device. In order to fabricate these components in a cost-effective manner on various substrates, the capability of the well-known sol-gel based material was analyzed in paper VI. For the realization of the functional axicon, material properties and processing parameters have to be customized.

2. Sol-gel chemistry

A sol is a colloidal suspension of solid particles in a liquid phase, in which the dispersed particles are small enough to remain suspended by Brownian motion [1–2]. A gel is a solid material network containing a liquid component, both of which are in a highly dispersed state [2]. In general, the sol-gel technique is described as a method in which solid materials, typically ceramics are formed via hydrolysis and condensation reactions from the molecular liquid phase.

Sol-gel method can be applied for the preparation of various types of materials. In order to achieve a wide range of material properties, most of the elements from the Periodic Table need to be available in a form suitable for sol-gel processing. Suitable precursors can be dissolved in a suitable solvent, typically an alcohol or other polar solvent, and they can react via hydrolysis and condensation reactions to the corresponding oxidic materials.

2.1 Alkoxide method

Most typical sol-gel precursors are metal alkoxides. Metal alkoxides have the general formula $M(OR)_x$, where M is a metal or a metalloid element and R is an alkyl or related group.

The applicability of metal alkoxides for the sol-gel technique is determined by their solubility, volatility (in order to purify the precursors) and their oligomerization capability. Oligomerization of the metal alkoxides affects the homogeneity of the final product. For example, in the case of antimony-doped tin dioxide coatings, the even distribution of antimony species in the tin dioxide lattice may be affected by the oligomerization of antimony alkoxides. In the worst case, antimony clusters are formed, leading to the loss of electrical properties in the final material. Fortunately, antimony alkoxides are volatile and soluble monomeric products [3].

2.1.1 Physical properties of metal alkoxides

The most important factors affecting the physical properties of metal alkoxides $[M(OR)_x]_n$ are the size and shape of the alkyl group (R), atomic radius, and the coordination number of the metal. Due to the high electronegativity of oxygen (3.5 in the Pauling scale), the metal-oxygen bonds ($M^{\delta+}–O^{\delta-}–C$), are expected to posses significant ionic character. However, most of the alkoxides show properties typical of the covalently bonded molecules, such as high volatility and solubility in common organic solvents. The factors affecting the decay of the polarity

in the metal-oxygen bond are (*i*) the inductive effect of the alkyl group, (*ii*) the presence of oxygen *p*-orbital to metal *d*-orbital π-bonding for early transition metals, and (*iii*) the formation of oligomeric species through alkoxo bridges of the type (Figure 1) [3]:

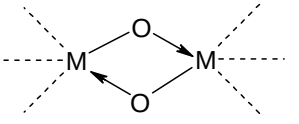

Figure 1. Alkoxo bridging in oligomeric metal alkoxides [3].

Oligomerization is a dominant feature of metal alkoxides unless inhibited by steric or electronic factors [3]. The extent of aggregation (*n*) is expected to decrease with the increase in size of the alkyl group, due to steric factors, and/or the presence of donor functionality in the alkoxo group, e.g. $OCH_2CH_2\mathbf{O}CH(CH_3)_2$. Moreover, it has been found that the extent of aggregation for almost all metals in the Periodic Table is dependent on the following considerations: (*i*) aggregation increases as the metal atom becomes more electron deficient; *(ii*) the larger the size of the metal atom, the greater the tendency to increase the degree of association; and *(iii*) increasing the steric demand of the alkyl group tends to decrease the aggregation [3]. In the case of methoxides, the unusually low volatility and solubility are explained by a combination of these factors and also by the high lattice energy between oligomers because of the small size of the methyl group [3].

In order to enhance the volatility and solubility of metal alkoxides, the ability of the metal and metalloid alkoxides to exchange the alkoxo groups with alcohols has been widely exploited. Reactions take place according to the general reaction 1:

$$M(OR)_x + nR`OH \leftrightarrow M(OR)_{x-n}(OR`)_n + nROH \uparrow \qquad (1)$$

There are three important factors that influence the extent of substitution in the alcohol interchange reactions: *(i*) the steric demands of the alkoxo groups (*OR* and *OR´*), *(ii*) the relative *O-H* bond energies of the reactant and product alcohols, and *(iii*) the relative bond strengths of the metal alkoxo bonds of the reactant and product alkoxides [3–4].

The ease of the interchange reaction increases from the tertiary to the secondary to the primary groups of the released alcohol due to the decreased steric hindrance [5]. The reaction from a more branched alkoxide structure to a less branched structure is sometimes more likely, if the product is significantly more associated than the reactant alcohol [3]. Relative pK_a values of the reacting and

leaving alcohol also affect the rate of the interchange reactions. If the pK_a value of the reacting alcohol is higher than that of leaving alcohol, the probability of the interchange increases [4].

Due to the wide use of alkoxy- and alkylalkoxysilanes in the sol-gel process, it is noteworthy to mention that the alcoholysis reactions of tetra-alkoxy silanes, $Si(OR)_4$, are generally very slow. On the other hand, alkyl alkoxysilanes appear to offer less steric hindrance to alcoholysis reactions, resulting in increased tendency for the alcohol interchange reactions [3].

2.1.2 Hydrolysis and condensation reactions

In general, the sol-gel technique is based on the hydrolysis of the metal alkoxide, and further condensation reactions of the fully and/or partially hydrolyzed alkoxides to corresponding oligomeric species. During hydrolysis, the alkoxide group in the metal alkoxide is replaced by the hydroxo ligand by the S_N2 type reaction (Eq. 2) [6].

$$M(OR)_x + H_2O \rightarrow HO\text{-}M(OR)_{x-1} + ROH \qquad (2)$$

The pathway of the hydrolysis has been presented in Figure 2 [7].

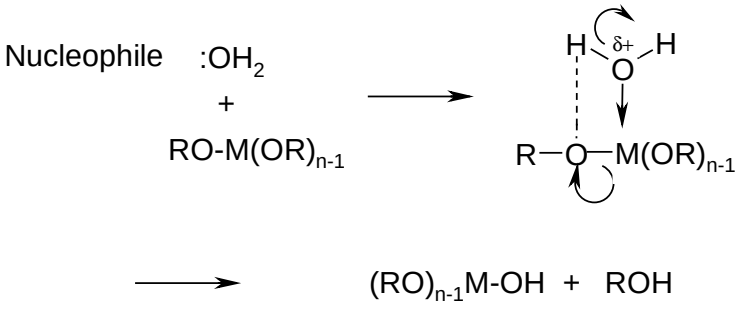

Figure 2. Schematic presentation for S_N2 type hydrolysis reaction [7].

The hydroxo metal alkoxide tends to react further with other hydroxo or alkoxo groups in the hydroxo metal alkoxides or metal alkoxides via condensation reactions (Eqs. 3 and 4) [6]:

$$(OH)_{x-1}M\text{-}OH + HO\text{-}M(OR)_{x-1} \rightarrow (OH)_{x-1}M\text{-}O\text{-}M(OR)_{x-1} + H_2O \qquad (3)$$

$$(OR)_{x-1}M\text{-}OH + RO\text{-}M(OR)_{x-1} \rightarrow (OR)_{x-1}M\text{-}O\text{-}M(OR)_{x-1} + ROH \qquad (4)$$

The dehydration process is presented in Eq. 3 and the dealcoholation reaction is shown in Eq. 4. During the sol-gel processing, the condensation reactions proceed further, leading to the formation of a three-dimensional network. At the gel point, the liquid sol is converted into a solid gel [8].

2.2 Salt method

Another widely used method is the salt method, in which inorganic salts are used as precursors. From an industrial point of view, the salt method is favored due to a much lower cost of metal salts when compared to alkoxides.

In the salt method, the sol is formed by dissolving the metal salts in water according to Eq. 5 [9].

$$M^{Z+} + :OH_2 \rightarrow [M \leftarrow OH_2]^{Z+} \quad (5)$$

The following equilibrium illustrates the dependence of the hydrolysis on the acidity of water and hence on the magnitude of the charge transfer Eq. 6 [9]:

$$[M(OH_2)]^{z+} \leftrightarrow [M\text{-}OH]^{(z-1)+} + H^+ \leftrightarrow [M{=}O]^{(z-2)+} + 2H^+ \quad (6)$$

The increased charge density on the metal, the number of metal ions bridged by hydroxo or oxo ions, and the number of hydrogens in ligand favor hydrolysis. The role of the anion during hydrolysis is described by the Mulliken electronegativity of the anion; if the electronegativity of the anion is approximately similar to that of water, χH_2O = 2.49 [10], it can substitute for all coordinated water molecules. Phosphates, $\chi H_2PO_4^-$ = 2.50 [10], and sulfates, $\chi HSO4^-$ = 2.64 [10], have this ability. If the electronegativity of an anion is close to that of water, as in the case of the nitrates, χNO_3^- = 2.76 [10], part of the water molecules are replaced. If the electronegativity is clearly higher, χClO_4^- = 2.86 [10], or smaller (e.g. Cl^-), anions cannot enter the coordination sphere of solvated cations [10]. The substitution of water molecules around the metal ions leads to the formation of new species with differing reactivities.

The particulate sol can be prepared by a condensation or a dispersion method. During condensation, particles are grown by a slow and controlled nucleation process, whereas in the dispersion method, particles are precipitated rapidly using the excess of base [2]. Stable sols are fabricated by peptizing or dispersing the particles in acids, where they are stabilized by positively charged surfaces. Gel can be formed via dehydration gelation, upon removal of water, or via alkaline gelation, upon increasing the pH of the sol [2].

2.3 Processing of the films

During the sol phase, films can be fabricated using common techniques such as dip-, spin-, or spray-coating methods. Depending on the nature of the solvent and the temperature and method used during the coating fabrication, most solvent is released from the fabricated film, resulting the gelation of the film. Same reactions that lead to gelation also lead to the syneresis of the material. Syneresis is a shrinkage process of the gel network resulting in the expulsion of liquid from the pores [11]. Syneresis leads to brittle materials, which crack easily during further film processing steps. The unwanted syneresis of the network can be diminished by aging or by using suitable covalently bonded organic groups in the inorganic material network. During the aging process, new metal-oxygen-metal bonds are formed via the condensation reactions [8].

Fabricated film achieves its final form during the drying and sintering processes. During the drying stage that can be performed thermally as well as by using IR- or UV-irradiation, water and alcohol content of the material is reduced. The evaporation of those species results in the porous structure. This, together with syneresis, is the main disadvantage of sol-gel processed materials when compared to bulk or films fabricated with traditional techniques. For example, the conductivity values and refractive indices of the conductive oxides are relatively far away from the bulk or traditionally fabricated materials, as described in chapter 3.2.4.

During sintering, the porosity of the formed material can be reduced. Sintering is typically performed thermally even though methods related to the use of lasers, energetic ions and microwaves have also been introduced. During sintering the material obtains its final form (glassy, crystalline, amorphous oxide etc.). However, too energetic or fast sintering processes lead to a highly porous or non-stoichiometric material structure.

2.4 Organically modified sol-gel materials

In inorganic-organic hybrid materials, material properties related to inorganic materials and organic materials are combined [12–14]. Typical inorganic properties are high temperature and chemical stability, hardness, brittleness, high stress, and low coefficient of thermal expansion, whereas properties such as elasticity, low stress, photoreactivity and high coefficient of thermal expansion are closely related to the organic materials. This type of combination of different kind of material properties offers extraordinary possibilities to fabricate multifunctional coating materials, which in general are complicated to produce by other methods.

2.4.1 Complexes prepared using metal alkoxides

One method of introducing organic functionalities into inorganic materials is the use of complexes where organic groups are attached to inorganic material via an oxygen bridge. In such cases *M-O-C* or a related bond have to be stable against hydrolysis or other reactions occurring during the sol-gel synthesis.

Due to the polarized metal-oxygen bonds in the direction $M^{\delta+}–O^{\delta-}–C$, metal atoms in metal alkoxides are susceptible to nucleophilic attack. The presence of vacant orbitals in metals, which can accept electrons from nucleophiles, and the oxygen atom susceptibility to electrophiles, render metal alkoxides highly reactive [7]. As already shown, metal alkoxide not only reacts readily with water and alcohol, but also with alkanolamines, carboxylic acids, β-diketones and β-diketoesters, Schiff bases, oximes hydroxylamines, and glycols [7].

The synthesis of complexes for the fabrication of hybrid inorganic-organic materials is mostly based on the reactions between carboxylic acids or β-diketones with metal alkoxides.

2.4.1.1 Reactions with carboxylic acids and acid anhydrides

Metal alkoxides react readily with carboxylic acids and acid anhydrides. During the reaction alkoxo groups are substituted for carboxylate groups as shown in Eqs. 7 and 8 [7]:

$$M(OR)_x + nR'COOH \rightarrow (R'COO)_nM(OR)_{x-n} + ROH \qquad (7)$$

$$M(OR)_x + nR'(CO)_2O \rightarrow (R'COO)_nM(OR)_{x-n} + nR'OOR \qquad (8)$$

Reactions of metal alkoxides with carboxylic acids are thermodynamically facile since carboxylate tend to act as bidentate ligands (Figure 3) [7]:

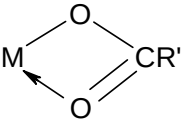

Figure 3. Bidentate binding in metal carboxylate [7].

Depending on the molar ratios, metal, and the nature of the reactive carboxylates and the leaving alkoxo group, the reaction yields metal alkoxide mono, di-, and tri- carboxylates. In most cases, homoleptic carboxylates are hard to obtain due to the decomposition of heteroleptic alkoxide carboxylates ($M(OR)_{x-y}(OOR')_y$) with increasing *y* to oxo-carboxylates and alkyl esters and eventually to oligomeric species [7].

2.4.1.2 Reactions of β-diketones

The enolic form of β-diketone (*R'C(O)CH=CH$_2$C(OH)R''*) contains a reactive hydroxy group, which reacts with metal alkoxides to yield mono- and bis-β-diketonate complexes according to Eq. 9,

$$M(OR)_x + yR'C(O)CH=CH_2C(OH)R'' \rightarrow$$

$$M(OR)_{x-y}(R'C(O)CH=CH_2C(O)R')_y + yROH \qquad (9)$$

where y = 1–2, and R' and R'' an alkyl or an aryl group [7,15–16].

The structure of bis-β-diketonate bis-alkoxide complexes is far more widely understood than the structure of corresponding carboxylates.

Structural analysis of bis-β-diketonate bis-alkoxide tin complexes have shown that alkoxo groups are mainly in *cis*-position surrounding the tin atom [15–16]. The *cis*-configuration is more stable than the *trans* configuration since RO^- ligands act as σ- and π-donors and π-bonding is most easily achieved if the alkoxo groups are located in *cis*-position [16]. Moreover, during the ^{119}Sn NMR studies of tin bis-isopropoxide bis-benzoylacetonate complexes major resonances contributed to *cis* isomers, whereas the resonances due to *trans* isomers showed intensities of only 6 % of the major peaks [15]. The possible *cis* and trans isomers for tin bis-alkoxo bis-β-diketonate complexes are shown in Figure 4. In compounds where R_1 differs from R_2, three major resonances corresponding to three possible *cis* isomers can be seen [15].

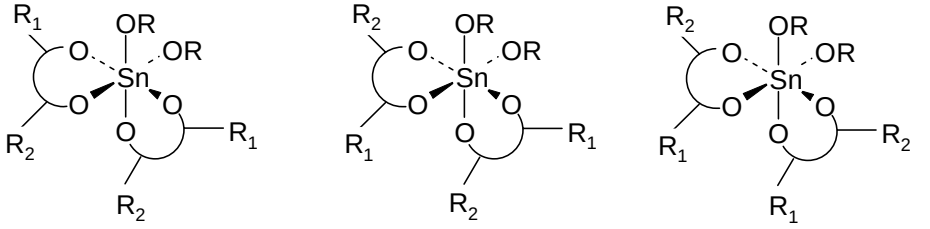

cis-Sn(β-diketonate)$_2$(OR)$_2$

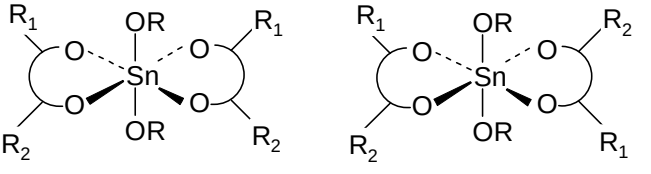

trans-Sn(β-diketonate)$_2$(OR)$_2$

Figure 4. Possible isomers for tin bis-alkoxo bis-β-diketonate complexes [15].

2.4.2 Organometallic route

Hybrid materials derived via the organometallic route are generally attributed to silicon alkoxide derivatives. Organometallic silicon alkoxides, in addition to alkoxo groups, contain an unhydrozylable $\equiv Si\text{-}C\text{-}$ bond ($R'_xSi(OR)_{4-x}$). Depending on the nature of R', it can behave as a network modifier or, if it is polymerizable, as a network former [17].

The network forming capability is typically obtained by using methacrylate or epoxy containing organic groups. These groups can be polymerized by radical or anionic polymerization, respectively. In Figures 5 and 6, organic network formation without cross-linkers is shown [18]. These reactions are also valid in materials where polymerizable groups are attached to the metal atoms via an oxygen bridge and therefore R in Figures 5 and 6 corresponds to metal or metalloid alkoxides bonded to the organic functionality via *M-C* or *M-O-C* bonds.

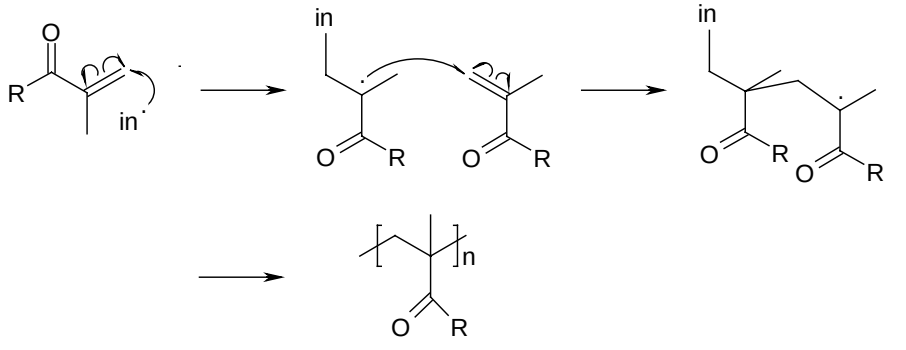

Figure 5. Polymethacrylate formation via radical polymerization [18].

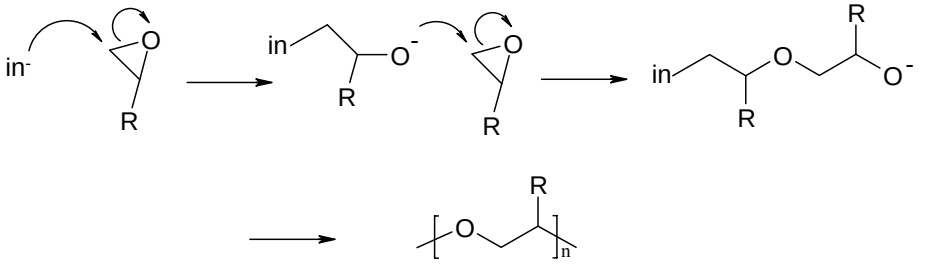

Figure 6. Anion initiated epoxy-ring opening [18].

Organic moieties can also behave as network modifying groups. These groups have a significant effect not only on the mechanical properties of the films, but also on the chemical nature of the material. For example, by appropriate choice of the organic functionality, materials or surfaces capable of antibody immobilization can be realized. These kind of materials contain organic moieties such as -$(CH_2)_3NH_2$,, -$(CH_2)_3SH$-$(CH_2)_3$ and $CH_2S(CH_2)_2CHO$ [17].

Another striking application of the use of organosilicon alkoxides is exploited by superhydrophobic or superhydrophilic surfaces. Superhydrophobicity can be achieved by the combination of fluorinated alkyl groups having a low surface energy and by using sol-gel derived nanoporous materials to increase air – liquid interface on liquid – film boundary [19]. Using a corresponding technique, such materials for sensor and sealing applications have already been realized in our laboratory (Figures 7 and 8).

Figure 7. A FESEM-image (field-emitting scanning electron microscope) of the nanoporous boehmite (AlOOH) surface derived from acetylacetone modified aluminum tri-sec-butoxide.

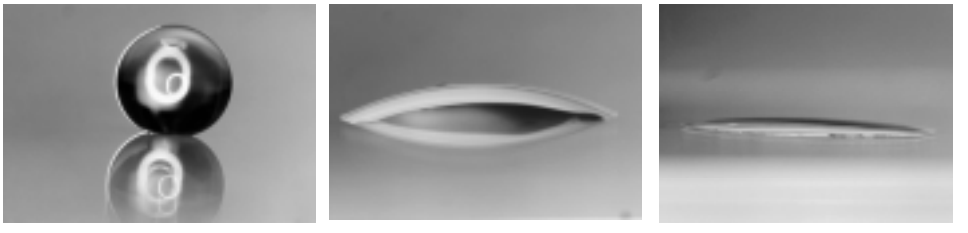

Figure 8. Superhydrophobic and superhydrophilic properties of the sol-gel derived materials. Left: a water droplet on a nanoporous fluoroalkyl silane surface. Middle: a water droplet on a soda-lime glass surface. Right: a water droplet on a nanoporous silane surface.

2.4.3 Organic moieties doped in the hybrid network

Organic materials can also be doped into the sol-gel matrix. In these types of materials, polymeric or monomeric molecules exist as a separate functional phase or molecule in an inorganic or inorganic-organic hybrid matrix. In order to achieve efficient doping, fabricated hybrid matrices have to be modified in such a way that molecules and polymers are soluble in the forming solid matrix in the required amounts to properly perform the desired functionality. Matrix effects, such as polarity, *pH*, ions etc., also have to be modified in such a way that they do not disturb the functionality of the active molecule. In some cases, the trapping of organic materials in a hybrid sol-gel derived network affects the properties of the organic material in a positive way [20].

3. Conductive tin dioxide coatings

Transparent conductive tin dioxide thin films have been attracting active interest since they can be used in many types of applications, especially in the field of optoelectronics [21]. Among optoelectronic applications, pure and doped tin dioxide thin films are potential candidates for transparent electrodes in display devices [22–23] and solar cells [23]. Furthermore, tin dioxide thin films can be used as gate electrodes for charge injection devices (CID) and charge-coupled devices (CCD) [23]. Other types of devices that can be realized using tin dioxide and its derivative films include heat mirrors [24], thin film resistors [23], transparent heating elements, touch sensitive switches, and applications in which microwave shielding or protection against the electrical discharge are required [21].

For all the above-mentioned applications, pure and doped tin dioxide thin films are alternative materials for the widely used tin doped indium oxide (ITO) coatings. The main advantage of tin dioxide thin films over ITO coatings is their price. Moreover, in comparison to other types of transparent conductors, excluding zinc oxide, the electrical properties of tin dioxide thin films are sensitive to different type of gases, including CO, CO_2, H_2S and alcohols [25]. Therefore, different types of tin dioxide thin films have also been attracting much interest in gas sensing devices.

During the next chapters, the basic features of pure and antimony-doped tin dioxide coatings are first presented. In chapter 3.2, commonly used methods for the sol-gel fabrication of the transparent conductive tin dioxide coatings are shown and compared to the coatings obtained with traditional techniques. During that chapter, the effect of argon-plasma treatment on the conductivities and optical transmission of the films is also presented. In chapter 3.3, a new method for the finely patterned, conductive and transparent antimony-doped tin dioxide structures is presented together with the precursor synthesis and characterization.

3.1 Properties

3.1.1 Tin dioxide

Tin dioxide is a degenerate n-type wide band gap semiconductor that has a direct optical band gap of 3.87–4.3 eV [23]. The transmittance of the tin dioxide at near-IR and visible wavelengths is high, typically over 80 % for thicknesses of a few hundred of nanometers, with plasma edge at about 3.2 μm. Tin dioxide,

cassiterite, has a tetragonal rutile type crystal structure. Tin dioxide thin films fabricated with different deposition techniques are typically polycrystalline, retaining the crystal structure of the bulk material. The preferred orientation of the crystallites, as well as the crystal size, are dependent on the precursor, deposition techniques and conditions.

The conductivity of undoped tin dioxide is determined by oxygen vacancies, the concentration of which is difficult to control. Furthermore, reducing or oxidizing atmospheres have been found to strongly affect the conductivity of pure tin dioxide [26]. Changes are attributed to the electron mobility (μ) rather than to the concentration of the charge carriers (N) [27]. This is caused by the chemisorption and desorption of oxygen from the grain boundary. Chemisorbed oxygen at the grain boundary forms a space of positively charged layer just below the surface of the tin dioxide and a potential barrier between the particles increases, leading to the decreased mobility of the electrons and hence to the reduced conductivity [25, 27]. Desorption of the oxygen from the grain boundary has an opposite effect on the electron mobility and electric conductivity. Due to these reasons, undoped tin dioxide thin films lack the thermal stability, and the doping of tin dioxide in order to introduce electron degeneracy and environmental stability is preferred [28].

3.1.2 Antimony-doped tin dioxide

The best dopant according to the conductivity values and optical characteristics of doped tin dioxide thin films is fluorine. Fluorine doping is, however, relatively hard to perform using sol-gel or other liquid phase deposition techniques, even though it has been reported in a few cases [29–30]. The most commonly used dopant for increasing the n-type conductivity of tin dioxide thin films is antimony. There are also numerous other dopants that have been used in order to increase the conductivity of tin dioxide thin films, for example *As*, *Mo*, *Ti*, and *P* [23, 31–32]. The effect of these alternative dopants on the conductivity values of tin dioxide thin films is negligible.

Sb^{5+} and Sn^{4+} cations have approximately the same ionic radii (0.71 Å and 0.65 Å, respectively) [33]. Therefore Sb^{5+} cations can easily be incorporated into the SnO_2 matrix by substitution of tin atoms with no discernible differences in the unit cell parameters [34]. Effective substitution of tin by antimony is also crucial in order to avoid the formation of solid solutions (e.g. Sb_2O_5-SnO_2) or mixed compounds with host oxide both affecting the conductivity of the material.

The dopant Sb^{5+} acts as a donor increasing the donor level by 35 meV [23], and hence shows the n-type conductivity. The increased carrier concentration shifts

the plasma edge from 3.2 μm (undoped tin dioxide) to 1.3 μm (tin dioxide doped with antimony) [34]. This occurs because the 'electron gas' (degenerated electrons) becomes reflective to radiation below its frequency [35]. Frequency (υ) is an increasing function of charge carriers *(N)* [35]. Because $\upsilon = c \cdot \lambda^{-1}$, where c is velocity of light, and λ is a wavelength, increasing carrier concentration, consequently, result in reflectivity at lower wavelengths. This is a common factor for transparent conductors as exemplified by the case of tin-doped indium oxide and fluorine-doped tin dioxide coatings [36]. Increased carrier concentration in antimony-doped tin dioxide thin films also causes a relatively large band gap broadening [31, 34], which is attributed to the Moss-Burstein effect [23].

Antimony has another stable oxidation state, +III. If the oxidation state of antimony is +III in a tin dioxide matrix, antimony dopant acts like an electron acceptor creating a hole, an electron trap, in n-type semiconductor and decreases the conductivity [23, 37].

The carrier mobility is restricted by ionized impurity scattering and grain boundary scattering [23]. Due to the ionized impurity scattering, the conductivity values start to decrease when the optimum doping level is exceeded. In most cases the optimum antimony-doping level is from 5 to 7 at.-%. Increase in the grain size due to the antimony-doping decreases the grain boundary potential through the film, and also the grain boundary scattering [23]. On the other hand, Sb^{5+} cations on grain boundaries induce a charged surface site. They produce a significant increase in the surface energy of the material, increasing the content of chemisorbed oxygen on the surface. This increases grain boundary scattering by increasing the grain boundary potential. Other factors assumed to be limiting factors for the conductivity of antimony-doped tin dioxides are the precipitation of Sb_2O_5 and the increased disorder [23].

3.2 Sol-gel derived tin dioxide coatings

Traditional deposition techniques for tin dioxide and antimony-doped tin dioxide thin films include atomic layer epitaxy (ALE), chemical vapor deposition (CVD), physical evaporation, spray pyrolysis and sputtering [31, 34, 38–39]. The possibilities to fabricate undoped and doped tin dioxide coatings using liquid phase deposition techniques, such as aerosol [40], sol-gel [41–42], and particulate methods [43], have been investigated since the 1980's.

3.2.1 Inorganic route

Due to the high solubility and low cost of the tin and antimony(III) chlorides, the majority of the tin dioxide and antimony-doped tin dioxide coating solutions (sols) have been prepared using the inorganic sol-gel method. The simplest way of fabricating the coating solutions is to dissolve tin and antimony chlorides ($SnCl_2{\cdot}2H_2O$, $SnCl_2(OCOCH_3)_2$, $SnCl_4$, $SnCl_4{\cdot}4H_2O$, $SnCl_4{\cdot}5H_2O$ and $SbCl_3$) separately in alcohol. After mixing and aging, the solutions can be deposited on substrates using dip-, spin- or spray-coating techniques [32, 42, 44–45].

During our research, we have used an even simpler approach [I, 46]. Coating solutions with the desired antimony-doping level were prepared simply by dissolving tin(IV) chloride tetrahydrate with a desired amount of antimony(III) chloride in ethanol. After refluxing, a small amount of Triton X-100 was added as a detergent to the solutions before the coating procedure. The drawback of all these direct salt methods is the easily vaporizable chlorine-containing tin and antimony compounds, which are lost during the early stages of the post treatment. This leads to inaccuracies in actual doping level determinations.

Another method is to fabricate sols by precipitating antimony ions containing $SnO(OH)_2$ from aqueous solutions using ammonium hydroxide. A stable coating solution can be achieved by peptizing the washed precipitation with ammonium hydroxide [47–48]. By using this technique, the formation of easily evaporating antimony-based compounds can be avoided. However, in this method, the actual antimony-doping concentration in the precipitate also differs from the theoretical value [48].

3.2.2 Coating solutions derived from alkoxides

Tin and antimony alkoxides are another group of widely used precursors, while conductive tin dioxide coatings using Sn-2-ethylhexanoate [49] and Sn(II)-citrate [50] precursors have also been produced. In the alkoxide method, tin alkoxides are generally first prepared from tin chlorides using salt elimination (Eqs 10 and 11) and base-catalyzed alcoholysis (Eqs 12 and 13) [4, 51–52]. At this stage, it has to be pointed out that the direct reaction between tin chlorides and alcohols does not lead to pure tin alkoxides, as assumed by Terrier *et al.* [53], but to the formation of mixed chloro-alkoxides [4, 7].

$$2SnCl_4 + 9NaOEt \rightarrow NaSn_2(OEt)_9 + 8NaCl \quad (10)$$

$$NaSn_2(OEt)_9 + HCl \rightarrow 2Sn(OEt)_4 + NaCl + EtOH \quad (11)$$

$$SnCl_4 + 2HNEt_2 \rightarrow SnCl_4(HNEt_2)_2 \quad (12)$$

$$SnCl_4(NHEt_2)_2 + 2NHEt_2 + 4HOR \rightarrow Sn(OR)_4 + 4H_2NEt_2 + Cl^- \quad (13)$$

A safer and better way is to use commercial tin and antimony alkoxides such as butoxides [54], isoproxides and ethoxides [41, 55] as well as ethylhexano-isopropoxide [49]. Some research groups have also used antimony chlorides together with tin alkoxides [56].

Coating solutions are usually prepared by dissolving the alkoxides in appropriate, preferably inert, solvents. In some cases, unhydrolyzed solutions are used as coating solutions [27, 52, 54] while hydrolysis of the alkoxides are also carried out. In order to prevent the precipitation of metals during the hydrolysis, suitable chelating ligands such as glycols, ethanolamines, β-diketones or carboxylic acids are generally used to reduce the hydrolyzation rate of tin alkoxides [41, 55]. Another technique has been the direct addition of water to the alkoxide solution. In that case, precipitation has been avoided by using strictly controlled amounts of water, or by using alkoxo ligands with a higher covalent character [51, 56].

3.2.3 Fabrication of pure and doped tin dioxide coatings

In order to achieve the conductive films, post treatment at elevated temperatures is required to crystallize the material and remove the organic or/and vaporizable inorganic moieties (chlorine containing species). The temperatures required for crystallization are typically around 400°C. High annealing temperature is a restriction, because organic substrates cannot be used. Furthermore, in the case of low glass transition temperature (T_g) glass substrates, barrier layers have to be used in order to prevent the diffusion of *Na*, *K* and *Ca* ions from glass to film. Another opportunity is to use High T_g substrates, such as boro-silicate or quartz.

3.2.4 Electrical properties of the Sol-gel deposited Sb:SnO_2 films

Even though sol-gel processing offers advantages such as homogeneity, purity, easy control of film thickness, the ability to coat large and complex surfaces [57], simple and cost-effective processing, and moreover the ability to produce ultrafine films [22, 58] it also has several disadvantages. The most crucial disadvantage is the low conductivity of the fabricated thin films, especially in the case of single layer coatings. In Table 1 typical electrical conductivities of antimony-doped tin dioxide coatings fabricated using different techniques are compared [31, 59].

Table 1. Typical conductivity values for antimony-doped tin dioxide thin films fabricated with different deposition techniques [31, 59].

Deposition technique	σ [S/cm]
CVD	1820
Evaporation	4000
Spray pyrolysis	1270
Sputtering	770
Sol-gel (single layer, 200 nm)	60
Sol-gel (10 layers, 200 nm)	250

The low conductivity values arise from the fact that sol-gel derived thin films are highly porous with small crystal sizes. However, by multiple coating – thermal annealing cycles, conductivity values of sol-gel fabricated pure and antimony-doped tin dioxide thin films can be increased. In Figure 9, the effect of multiple coating – thermal annealing cycles to the resistivity values, which are inverse values of conductivities, of antimony-doped (6.9 at.-%) tin dioxide thin films is presented. Films are fabricated using the deposition solutions prepared according to our sol-gel salt method [I, 46].

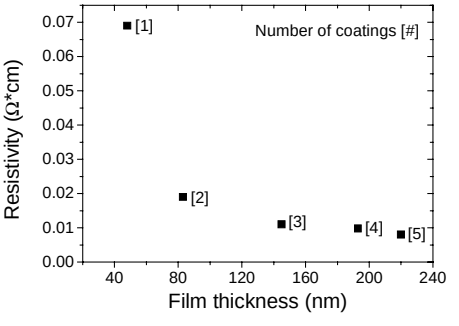

Figure 9. The effect of multiple deposition – heat treatment cycles on the electrical resistivity of sol-gel salt method fabricated thin films [46].

According to Figure 9, the resistivity does not decrease linearly with increasing film thickness (i.e. precisely increase number of layers). A similar trend in resistivity with increasing film thickness has also been reported earlier [22, 42]. This behavior has been explained in terms of layer morphology. The layer cross-section, analyzed by TEM, shows that each individual layer consists of a denser interface lying on the top of more porous material. This denser fraction decreases the overall resistivity of the coating [42]. It has been noted that the pores of the first layer will be filled when the second layer is applied [22]. It can be

assumed that the decrease in resistivity depends on both mechanisms, because the difference of resistivities between the first and second layer is so drastic (see Figure 9). After the deposition of the second layer, the decrease of film resistivity is almost linear.

The effect of different precursors, heat treatment techniques, and the CO_2 laser densification on the electrical properties of antimony-doped tin dioxide thin films have widely been investigated by Gasparro *et al.* [59]. During their investigation they observed that the stabilization of salt method fabricated coating solution is required. This is due to the high chlorine content of the solution, which leads to the formation of volatile antimony and tin compounds, which are lost during the early stages of the sintering process. Films prepared with the alkoxide method do not show a similar effect. It was also observed that films fabricated using the spray pyrolysis technique have larger grain size when compared to sol-gel fabricated films. This leads to higher carrier concentration and mobility when compared to smooth and porous sol-gel derived films [59]. However, the porosity of the sol-gel-derived films can be reduced using CO_2 laser irradiation. This leads to denser structure in comparison to thermally treated films and hence to better conductivity. Canut *et al*. [60] have also investigated the possibilities to increase the density of sol-gel fabricated antimony-doped tin dioxide thin films. They observed that by using 300 keV Xe^+ ions at fluences up to $4 \cdot 10^{15}$ cm^{-2}, the density of single layers increases from 38 % to 82 % of the bulk tin dioxide density.

Another factor affecting the conductivity of the sol-gel derived antimony-doped tin dioxide thin films is the oxidation state of the antimony. Terrier *et al.* [61] have investigated the oxidation states of antimony in the tin dioxide fabricated by sol-gel salt method. Their measurements indicate the presence of two oxidation states for antimony. Antimony occurs as Sb^{5+} with low antimony-doping concentrations. As antimony-doping concentration increases, the Sb^{3+} species overcomes Sb^{5+}. The presence of two oxidation states has also been found by other authors using different methods [33, 62]. The presence of Sb^{3+} in a Sb^{5+} doped tin dioxide matrix leads to the compensation of the electron degeneracy created by Sb^{5+}, thus leading to reduced conductivity. Another contradictory observation was that the crystal size decreases as the antimony-doping level increases. This is understandable in terms of increased stress at the tin dioxide matrix due to the different oxidation state and ion size of the antimony dopant [61], but antimony-doped tin dioxide thin films fabricated using different deposition techniques, including the sol-gel method, have been widely reported to have larger crystallite size when compared to undoped films [III, 23, 41].

It can be concluded that the main problem related to the sol-gel derived pure and antimony-doped tin dioxide thin films is their high porosity. This leads to relatively low conductivity values when compared to films deposited by other techniques and also to low refractive indices (1.6–1.8) when compared to bulk tin dioxide (2.2). The transmission values of pure and antimony-doped tin dioxide thin films are comparable to or better than those of thin films fabricated using other techniques. As described above, methods of increasing electrical conductivities during the sintering are under extensive investigation.

3.2.5 Post-treatment techniques

Although fabrication of tin dioxide and antimony-doped tin dioxide thin films have been studied carefully, there are relatively few reports about the possibilities to enhance the electrical properties of sol-gel prepared tin dioxides after the final film formation. *Sentugguvan and Malhotra* investigated the effect of different atmospheres during the annealing and also the effect of post treatment at hydrogen plasma on the conductivity of pure and antimony-doped tin dioxide thin films [28]. They observed that the vacuum and hydrogen annealing increases both carrier concentration and carrier mobility and hence results in the increase in the conductivity values of antimony-doped (3–7 at.-%) tin dioxide thin films by one to two orders of magnitude. Annealing in oxygen and argon atmospheres has the opposite effect on the conductivity.

We have investigated the effect of argon-plasma post treatment on the electrical conductivities of antimony-doped tin dioxide thin films [I]. Argon-plasma can be expected to increase the electrical conductivity of the thin films by removing the depletion layer and increasing the amount of oxygen vacancies.

The antimony-doped (theoretical *Sb* of 13.8 at.-%, in order to obtain maximum conductivity) tin dioxide sols were prepared as described earlier [I,46]. The thin film coatings were deposited on borosilicate glass substrates. Films were prepared by the spin-coating method. Films were allowed to dry in a stabilized atmosphere at a relative humidity of 45% and a temperature of 25°C and then dried at 150°C for 30 minutes. The drying stage was immediately followed by sintering in a belt furnace in an air atmosphere (maximum 620°C for 20 minutes). The deposition procedure was repeated three times to increase the thickness of the film after which the films were argon-plasma treated [I].

The conductivity measurements clearly show that argon-plasma treatment increases the electrical conductivity of thin antimony-doped tin dioxide films. The maximum increase in conductivity was found in films treated in argon-plasma for 20–75 minutes, from 138 to 400 (S/cm). Thus, sol-gel fabricated antimony-

doped tin dioxide films may be said to be highly sensitive to argon-plasma. The achieved conductivity is, however, not stable under ambient conditions, but starts to decrease immediately after removal from the plasma chamber [I]. It can be concluded that argon-plasma can be used in the production of conductive tin dioxide coatings in order to improve the batch-to-batch reliability of the electrical properties of thin films. However, coatings have to be protected from ambient atmosphere conditions.

We have also investigated the effect of argon-plasma treatment on optical properties of the undoped and 5 at.-% antimony-doped samples [63]. Also in this case, the argon-plasma treatment of the fabricated antimony-doped and undoped tin dioxide films has a drastic effect not only on their electrical, but also on their optical properties. The conductivity of these films increases over two orders of magnitude for undoped and 450 % for 5 at.-% antimony-doped tin dioxide thin films. The optical transmissions decrease 14 % and 10 % at 550 nm respectively, as shown in Figures 10a and 10b. Optical transmission returned to the original level when samples were stored at ambient atmosphere

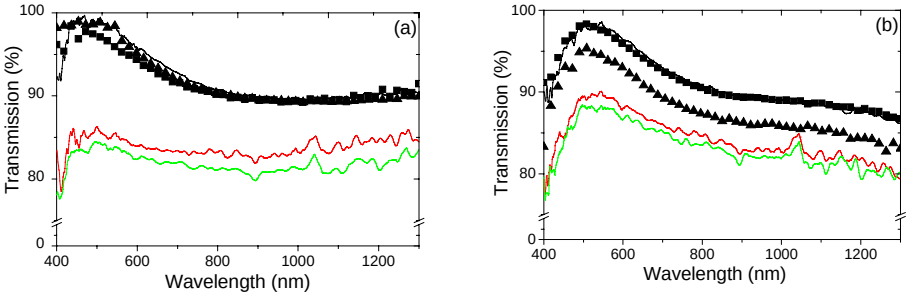

Figure 10. a) SnO_2 and b) Sb:SnO_2 (5 at.-% Sb) transmissions as a function of the plasma exposure: black line untreated, red line 60 s and green line 300 s. ▲ and ■ indicate transmittances 50 and 170 hours after the longest plasma exposure, respectively [63].

3.3 Directly photopatternable tin dioxide thin films

Patterning of film is needed in applications utilizing transparent conductive undoped and antimony-doped tin dioxide thin films. Due to the high chemical durability of tin dioxide [64–65], fine patterning of tin dioxide thin films by wet etching has been reported to be rather complicated. Although dry etching patterning has been successfully demonstrated, it is usually a time-consuming multi-step processes, capital expensive, substrate size limited and requires spe-

cial equipment. Therefore ITO coatings are favored over conductive tin dioxide thin films. However, the electrical and optical properties of ITO are not ideal for all proposed applications, especially for transparent cathodes in organic light emitting diodes (OLED) [66]. For those applications, pure and antimony-doped tin dioxide thin films are cost-effective alternatives. Accordingly, new material approaches for fast and cost-effective fine patterning of tin dioxide and its derivative thin films are required.

In order to resolve the problems related to the fine patterning of pure and doped tin dioxide thin films, a new approach employing a combination of direct photolithographic processing of liquid phase deposited organo-tin films, followed by thermal annealing has been reported to be successful. Conductive tin dioxide structures and, in our case, antimony-doped tin dioxides have been fabricated by using photo-reactive poly(4-((trimethylstannyl)methyl)styrene) [64], acetyl acetone modified tin(II) chloride [65], n-phelyldiethanolamine modified tin 2-propoxide [67], and methacrylic acid or benzoylacetone modified, antimony-doped tin alkoxides [II–IV]. A similar strategy has also been utilized in order to fabricate directly photopatternable ITO coatings via the modification of indium 2-propoxide with benzoic acid [68].

3.3.1 Synthesis and film fabrication

3.3.1.1 Methacrylic acid modified precursors

Our first approach was to synthesize the directly photopatternable pure and antimony-doped tin dioxide materials by direct reaction between methacrylic acid with tin and antimony alkoxide solutions [II–III]. Formed complexes can be polymerized via UV-induced radical polymerization as shown in Figure 5. Due to the polymerization UV-irradiated areas have lower solubility in comparison to unexposed areas; negative tone behavior.

As a first step, the tin(IV) isopropoxide and antimony(III) isopropoxide were dissolved separately in dry 2-isopropoxyethanol (2-IPE). In order to obtain the desired antimony-doping level (1–10 at.-%), a suitable amount of antimony alkoxide solution was added and subsequently mixed well with the tin alkoxide solution. Methacrylic acid was added to the metal alkoxide solution. The amount of the added methacrylic acid needs to be twice the amount of tin and antimony alkoxides in order to fabricate directly photopatternable films.

IR-spectroscopic analysis (see Figure 11) clearly showed the formation of methacrylic acid modified tin alkoxides. The IR spectrum of pure methacrylic

acid showed carboxylic band, *i.e. C=O* stretching band at 1716 cm^{-1}. In the spectrum of the synthesized complexes of tin(IV) isopropoxide and methacrylic acid, the intensity of the carboxylic band of methacrylic acid was significantly decreased. Furthermore, two new bands appeared at 1535 and 1416 cm^{-1} indicating the formation of an oxalate, in which the *C–O* bond order is 1.5 [69–70]. The residual *–COOH* peaks (around 1716 cm^{-1}) in the IR spectrum of the reaction product indicate that part of the methacrylic acid did not react with tin(IV) alkoxide. Another possibility is that in the liquid phase, chemical equilibrium between unsubstituted, and mono- and di-methacrylic acid substituted tin alkoxide species occurs. This equilibrium has also been reported to occur with β-diketone modified tin alkoxides [15].

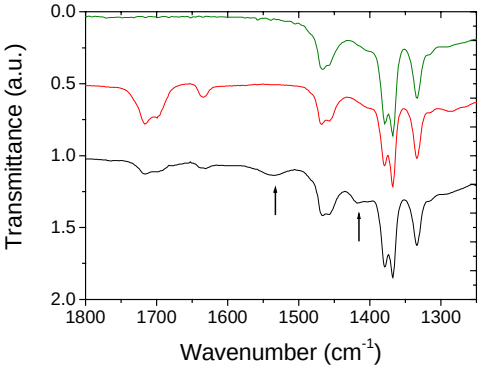

Figure 11. IR-spectra of tin(IV) isopropoxide (green), methacrylic acid (red) and tin(IV) isopropoxide and methacrylic acid (black) in 2-isopropoxyethanol [70].

Mass spectroscopic analysis (ESI-TOF) supports the latter possibility by showing unreacted, mono- and bis-methacrylic acid substituted tin methoxide compounds both in the positive and negative mode, see Table 2. [70]. Methanol was used instead of 2-IPE during the mass spectroscopic analysis due to the equipment requirements. Compound identifications were also verified by high precision mass measurements for ions producing peaks at m/z 321 and 375.

Table 2. Peaks in ESI-TOF mass spectra of methacrylic acid modified reaction mixture [70].

m/z	Identification
Positive ion mode	
267	$[Sn(OMe)_4Na]^+$
321	$[Sn(OMe)_3OOCC(CH_3)CH_2Na]^+$
375	$[Sn(OMe)_2(OOCC(CH_3)CH2)_2Na]^+$
Negative ion mode	
275	$[Sn(OMe)_4(OMe)]^-$
283	$[Sn(OMe)_4(Na)(H_2O)\ -2H]^-$
329	$[Sn(OMe)_3OOCC(CH_3)CH_2(OMe)]^-$

The reaction between tin(IV) isopropoxide, methanol and methacrylic acid, carried out in dry hexane with molar ratios of 1:4:2, respectively, yields products which can be crystallized at -18°C [71]. Unfortunately, we have not been able to determine the crystal structure yet, but the ^{119}Sn solid state MAS NMR spectrum was acquired from powdered crystals. Chemical shifts were referenced to standard $Sn(CH_3)_4$ scale by calibrating the shifts using SnO_2 as a standard (δ = –603 ppm). The solid state ^{119}Sn MAS NMR spectrum shows one signal with the chemical shift –691 ppm that is typical for tin coordinated with six oxygen nuclei. The solution ^{1}H NMR spectra were additionally acquired in deuterated dimethyl sulfoxide (*DMSO-d*^{6}). Chemical shifts were reported relative to trimethyl silane (*TMS*). Interestingly, in the ^{1}H NMR spectrum of dissolved crystals, we obtained, together with methoxy and methacrylic acid signals, a doublet at 1.06 ppm (J_{HH} = 6.1 Hz) and septet at 3.77 ppm (J_{HH} = 6.1 Hz) corresponding to isopropoxide protons. This observation clearly indicates that in the presence of several possible ligand molecules, the metal alkoxide chemistry is much more complicated than commonly assumed.

Suitable photoresponse for coating solution (prepared using 2-isopropoxyethanol (2-IPE)), was achieved by dissolving 2 wt.-% of a radical UV-photoinitiator, Irgacure 819 (Ciba), with respect to methacrylic acid into the synthesized solutions. Pure and antimony-doped tin dioxide thin films were produced by the spin-coating method. After the spin coating, the films were patterned by using a binary photomask and the UV-irradiation from a mercury UV-source (10 mW/cm^2 at 365 nm). UV-doses between 300 and 400 mJ/cm^2 have been used. Isopropanol, containing less than 0.1 % water, was used as a developer. After development, patterned organo tin polymer was thermally annealed onto the crystalline, pure or antimony-doped tin dioxide in ambient atmosphere at elevated temperature. The highest temperature during the thermal annealing of the samples was 560°C for 20 minutes. The differential scanning calorimeter (DSC)

measurements indicate that the crystallization of these materials occurs between 390°C and 415°C, the temperature being lower both the for photopatterned and the antimony-doped samples [III]. In Figures 12a and 12b the fabricated thin film structures are presented. The smallest feature size during the experiments was 3 µm [II].

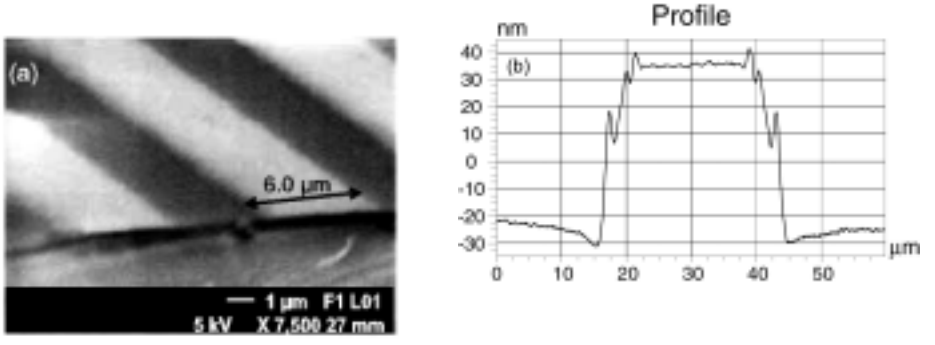

Figure 12. Fabricated thin film structures. a) Presents a SEM image of a patterned grating structure with 6 µm line width. b) A cross sectional profile (Wyko NT 2000) of a conductor line with 25 µm line width [II].

3.3.1.2 Benzoylacetone modified precursors

In order to investigate the possibilities to fabricate patterned antimony-doped tin dioxide thin films using other types of photoreactive ligands and moreover, to examine the effect of the used ligand on the conductivity values of the films, we also synthesized *β*-diketonate modified tin alkoxide precursors [IV].

It is widely known that *β*-diketones form bidental chelate rings with the central metal atom in metal alkoxides by replacing the existing alkoxy ligand [16]. Chelate rings show absorption bands at UV wavelengths, which are characteristic of the π-π^* transitions [72]. The UV-irradiation dissociates the chelate bonds and simultaneously decreases the solubility of the material in solvents such as alcohols, ketones or acids. Tohge *et al.* have done pioneering work in this field, and they have successfully demonstrated the formation of directly UV-photopatternable Al_2O_3-SiO_2 [73], Al_2O_3 [74], ZrO_2 [75], and *PLZT* (lead-lanthanide-zirconium-titanate) [76], thin films using *β*-diketonate modified metal alkoxides.

The synthesis of the photoreactive benzoylacetone modified tin alkoxides was performed in a two stage procedure [IV]. Tin(IV) t-butoxide, antimony(III) 2-propoxide and benzoylacetone were used as a precursors. During the first stage,

t-butoxide ligands of tin and antimony precursors were replaced with 2-isopropoxyethoxy ligands (OIPE). The ligand exchange reactions were confirmed using ^{1}H & ^{13}C NMR and mass spectroscopic techniques. In the second stage, benzoylacetone modification was performed by adding benzoylacetone (dissolved in 2-IPE) drop-wise into the pure $Sn(OIPE)_4$ and $Sb(OIPE)_3$ doped solutions. The molar ratio of benzoylacetone has to be twice the amount of used metal alkoxides in order to obtain the direct UV-photopatternability. The concentrations of the fabricated solutions were 0.5 M (*Sn+Sb*) in every case. Solutions were allowed to react for 24 hours, after which they were used during 24 hours.

Tin(IV) 2-isopropoxyethoxides were characterized using ^{1}H, ^{13}C and ^{119}Sn NMR techniques [77]. The ^{119}Sn NMR spectrum of pure tin(IV) 2-isopropoxyethoxide (in deutered chloroform, $CDCl_3$, 273 K) shows a big, sharp peak at -629 ppm and also a very small, sharp peak at -617 ppm (relative to tetramethyl tin, $Sn(CH_3)_3$), both corresponding to a six-coordinated tin atom. When temperature is increased to 295 K, the peaks are broader, having approximately the same integrated areas. When temperature is decreased to 320 K, the integrated areas are the same but the peak at -617 ppm is sharp and the peak at -629 ppm broad. The only difference at ^{1}H NMR spectra is the increasing resolution towards higher temperatures. In ^{13}C -{^{1}H}-NMR, the spectra peaks are sharper at higher temperatures, but there are also small peaks at lower temperature in CH/CH_2 region. The obtained results indicate two different tin environments, probably due to the oligomerization or presence of different type of isomers.

Interestingly when synthesized tin(IV) 2-isopropoxyethoxide [IV] is reacted with methacrylic acid in hexane, all 2-isopropoxyethoxide ligands were replaced by methacrylic ligands resulting in $Sn(OOCCH(CH_3)CH_2)_4$. ^{119}Sn NMR spectrum (in $CDCl_3$) showed only one eight-coordinated tin atom at -873 ppm. ^{1}H and ^{13}C -{^{1}H}-NMR spectra acquired in $CDCl_3$ showed only one type of signal identified to methacrylic acid.

In the ^{119}Sn spectrum of synthesized benzoylacetone modified tin(IV) 2-isopropoxyethoxide, three peaks at -693.4, -693.8 and -694.6 can be recognized from fresh and 7 day-old samples. These peaks correspond to *cis*-isomers of bis-benzoylacetone bis-2-isopropoxyethoxide tin (as shown in Figure 4) with integrated areas of 28 %, 52 % and 20 %, respectively. The same signals with four additional trans-isomer signals, whose intensity was about 6 % from *cis*-isomers, has been obtained with bis-benzoylacetone bis-2-isopropoxide tin [15] (see Figure 4). The existence of four *trans*-isomers is not clear, even though assumptions to association can be presented. When our solutions were aged (older than 12 days), weak signals (signal to noise ratio only 1:1) appeared corresponding to

trans-isomers. In ^{13}C -{^{1}H}-NMR spectra peaks corresponding to 2-isopropoxyethoxy and benzoylacetone ligands were recognized.

In this case, UV-photopatternable pure and antimony-doped organo-tin films were also fabricated by the spin-coating method. The required UV-reactivity was achieved by drying the films at 100°C for 10 minutes. For the structure patterning, films were UV-exposed using a contact binary mask and UV-dose of 7.2 J/cm^2 (at 365 nm). Figure 13 presents the effect of 7.2 J/cm^2 UV-irradiation to the absorption of chelate ring [IV].

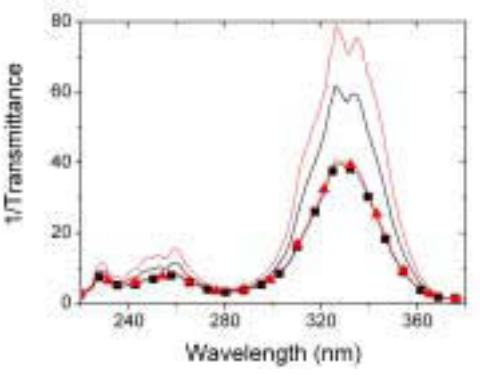

Figure 13. UV-spectra of unexposed and UV-irradiated pure and Sb-doped samples, in which the BzAc vs. metal alkoxide ratio was 2. The black line corresponds to undoped and the red line to 5 atl.-% Sb doped unexposed samples. Black (—■—) corresponds to undoped and red (—■—) to 5 at.-% Sb doped UV-irradiated (7.2 J/cm^2) samples [IV].

After UV-irradiation, the unexposed parts, i.e. the more dissolvable regions, were removed in an acetone bath. Films were annealed in air at 560°C for 20 minutes in order to crystallize the films and remove the organics. Figure 14 presents a Wyko NT 3300 3D, white light optical interferometer image from the patterned structure of a 25 µm wide line structure after the thermal treatment [IV].

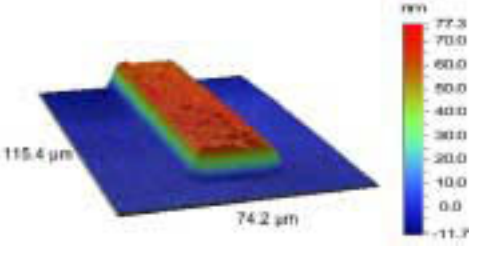

Figure 14. White light optical interferometer image from a patterned structure after the thermal treatment. Line width is 25 µm [IV].

3.3.2 Electrical properties

The optical transmissions were found to be over 85 % for all fabricated films (50–100 nm) at visible wavelengths. Table 3 shows the electrical characteristics of the fabricated single layered films with and without UV-irradiation [II–IV].

Table 3. Conductivities of unexposed and UV-irradiated pure and antimony-doped tin dioxide single-layered coatings derived from methacrylic acid and benzoylacetone modified precursors [II–IV].

Methacrylic acid modified precursors			**Benzoylacetone modified precursors**		
	Conductivity (S/cm)			Conductivity (S/cm)	
Sb (at.-%)	Unexposed	UV-irradiated (0.3 J/cm^2)	Sb (at.-%)	Unexposed	UV-irradiated (7.2 J/cm^2)
0	0.02	0.3	0	0.005	0.007
1	1.2	4.9	1	4.8	5.9
5	5.4	13.8	5	17	17.2
10	2.0	3.3	10	9.3	7.8

According to conductivity values given in Table 3, UV-irradiated samples derived from methacrylic acid modified precursors have higher electrical conductivity with all doping levels when compared to unexposed samples. The biggest relative increase in the conductivity was obtained in the case of undoped samples (0.02 S/cm → 0.3 S/cm, 1500 %). The lowest magnitude of increase was found for the highest investigated antimony-doping level (*Sb* 10 at.-%, 2.0 S/cm → 3.3 S/cm, 60 %). The reasons for this were found during the (powder x-ray diffraction) XRD and (x-ray photon spectroscopy) XPS measurements [III].

According to the XRD diagram of the prepared powders, all samples were polycrystalline and correspond to the SnO_2 structure (Figure 15) [III]. However, the crystal size of the unexposed samples was found to increase with increasing antimony-doping level from 10 nm for pure tin dioxide to 15 nm and 25 nm for 1 at.-% and 5 at.-% antimony-doped tin dioxide, respectively [III]. On the other hand, the crystal sizes of all analyzed UV-irradiated samples were approximately 25 nm. Consequently, it follows that the polymerization of the methacrylic ligands assists the crystallization of the samples.

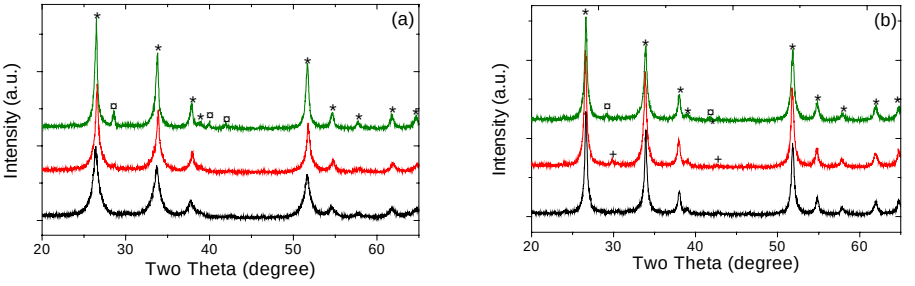

*Figure 15. XRD diagram of a) unexposed and b) UV-irradiated pure and Sb-doped tin dioxide powders. The black line corresponds to Sb doping level at 0 at.-%, The red line 1 at.-% and green 5 at.-%. Patterns marked by *, ¤ and + correspond to cassiterite [ICDD number 71-0652], elemental antimony [05-0562] and tin monoxide [72-1012 and 24-1342]], respectively [III].*

Measurements were performed in order to be sure that UV-irradiation has the same kind of effect on the crystal size of thin film samples as in the case of powdered samples atomic force microscopy (AFM). From the AFM-measurements [III] it can be concluded that the UV-irradiation has a remarkable affect on the surface morphology of the undoped tin dioxide surfaces. There is a small difference at the R_{rms} (root mean square roughness = average of the height deviations and the mean surface) values of the UV-irradiated sample (0.263 nm) when compared to unexposed samples (0.214 nm). A bigger difference can be seen in R_{pv} (peak-to-valley roughness = maximum vertical height deviation) values. R_{pv} for UV-irradiated samples were 2.353 nm. The corresponding value for the unexposed sample was 1.834 nm [III]. In the case of 5 at.-% antimony-doped samples, the differences between unexposed and UV-irradiated are negligible. UV-irradiated surfaces look even smoother than in the case of undoped samples and grain size increase cannot be seen. Observations during the surface morphology analysis clearly indicate that the corresponding behavior (crystal size) to the powder samples also occurs in the case of thin film samples [III].

Only *C*, *O*, *Sb* and *Sn* were detected in the X-ray photoelectron spectroscopy (XPS) spectra recorded from annealed film surfaces. The carbon content and the C 1s line shape were typical of the surface contamination detected in air-exposed oxide surfaces. Furthermore, the C 1s line disappeared completely during the first sputter cycles. Sputter profiles for oxygen, tin and antimony indicated homogenous elemental distributions throughout the film, apart from the outermost surface, where the relative oxygen content was somewhat higher. Oxygen-to-metal atomic ratios *O/(Sn+Sb)* were found to increase with increasing *Sb* doping level from 2 to 2.6, which is lower than expected from the higher oxygen content of the *Sb*-oxide alone. This could be attributed to changes in film composition,

but it would also be enhanced by changes in surface energy due to the increasing *Sb* content, which would increase the level of surface *OH* groups. Another interesting observation was that throughout the series, both the *Sb/(Sb+Sn)* and *O/(Sb+Sn)* ratios on the surface of the UV irradiated films were slightly lower than those in the unexposed films. The UV irradiation seemed to facilitate a more even distribution of *Sb* throughout the material, while a slight surface enrichment is observed in the unexposed samples [III].

The XPS data indicates that UV-irradiation has a small but detectable effect on the amounts of *Sb* and *O* on the surface of the samples. The lower amount of *Sb* on the surface of the UV-irradiated samples may be attributed to lowered mobility of the *Sb* in the material, resulting in more even distribution of *Sb* through the films. This assumption may explain some of the differences between the conductivities of the unexposed and the UV-irradiated samples [III].

In conclusion it can be said that the observed increase in grain size explains the differences in the conductivities of the unexposed and UV-irradiated thin films prepared from *methacrylic acid modified tin alkoxides*. The increase of the crystal size at low doping levels reduces the electron scattering at grain boundaries and hence increases the mobility of the carriers as well as the conductivity. For the samples with higher doping levels, this phenomenon does not cause an increase in the conductivity values, as there is no significant difference in grain size between unexposed and UV-irradiated samples. Due to this, the observed increase in the conductivity values of the UV-irradiated samples with higher doping levels may be attributed to the more even antimony distribution of the UV-irradiated films, as suggested by the XPS analysis. On the other hand, it can be seen from the values given in Table 3 that UV-irradiation has only a slight effect on the conductivities in the case of films fabricated from *benzoylacetone modified precursors*. A similar systematic increase in the conductivity values, as in the case of films derived from methacrylic acid modified tin alkoxides, cannot be seen. However, the conductivity values of these films are little bit higher, but still a couple of orders of magnitude lower than the desired conductivity values obtained with traditional coating techniques (10^3 S/cm).

4. Materials for optical protection and micro-optics

4.1 Laser protective eyewear

Protection of human eye and optronic devices against laser radiation has become essential due to the wide use of lasers in both military and commercial applications. Laser eye protection requires high optical density at laser threat wavelengths and high transmittance at wavelengths where the device or eye (400–750 nm) is functional. The most dangerous wavelength region for the human eye is in the near-infrared (NIR), 750–1400 nm. At those wavelengths invisible to human eye, the shutter reflex of the eye is not functional. Furthermore, NIR wavelengths are also focused by the lens on the retina of the eye, increasing the retinal laser power density by five orders of magnitudes corresponding to the corneal power density.

In addition to high optical density at laser threat wavelengths and high visible transmission, protective eye-wear for military applications has to be mechanically tolerant, its laser protective effect can not be angle dependent, it has to prove satisfactory ballistic protection and it has to be cheap and suitable for mass production. These requirements restrict the use of conventional laser protective methods e.g. interference coatings, optically nonlinear molecules [78] and incorporation of absorption molecules into an organic polymer matrix [79].

The multifunctional sol-gel coatings offer a feasible way to achieve laser protective properties and mechanically tolerant surfaces with one coating. Different types of laser dye molecules trapped into inorganic and hybrid sol-gel matrices have been already realized [80–81]. The liquid phase processing of the sol-gel materials provides an adequate way of mixing the dyes into the final solid matrix, resulting in a homogeneously doped material. Furthermore, by varying the chemical nature of the formed matrix via organic network modifying groups, the solubility of the dyes in the inorganic or hybrid matrix can be enhanced, resulting in sufficient concentration of the dye molecules. Solubility of the dye molecules in sol-gel matrix is also essential in order to avoid the aggregation of the molecules, which leads to insufficient optical properties [78].

4.1.1 Mechanically tolerant sol-gel coatings

SiO_2 films derived from tetra-alkoxy silanes not only have properties related to a three-dimensional SiO_2 network, but also porous structure typical of sol-gel

processed materials. These properties include optical clarity at visible wavelengths, hardness, brittleness and low thermal expansion coefficient. For the fabrication of mechanical protective coatings on plastic substrates, brittleness has to be reduced and the thermal expansion coefficient has to be fixed at the level of the used plastic substrate. By introducing organic functionalities to the porous sol-gel derived SiO_2 matrix, the above requirements together with denser structures can be achieved at relatively low temperatures [17, 82]. Since the middle of the 1980's, organic-inorganic hybrid materials have been developed for the mechanical protection of plastic substrates [14, 17, 82–86]. These mechanically tolerant sol-gel fabricated hard coatings have been typically produced either by polymer or particulate methods.

4.1.1.1 Polymeric method

In the polymer type of synthesis, an inorganic backbone is constructed by using polymerizable alkyl chain containing silicon trialkoxides and metal, typically *Ti*, *Zr* and *Al*, alkoxides. The incorporation of metal species in the SiO_2 network leads to a denser inorganic backbone and hence increased mechanical properties [12]. However, the incorporation of metal species homogeneously in SiO_2 network via hydrolysis and condensation reactions is rather difficult to perform due to the different reactivities of silicon and metal alkoxides. Therefore, an advanced method of overcoming the precipitation of metal species during the plain water addition in mixed alkoxide solution has been developed. During the chemically controlled condensation (CCC) method hydrolysis and condensation reactions are controlled precisely by chemical water generation within the system [12]. The water is produced by an ester formation in which the water molecule is formed during the reaction between solvent alcohol and carboxylic acid (Eq. 14):

$$\mathrm{ROH + R'COOH \xrightarrow{H^+} R'COOR + H_2O} \qquad (14)$$

The formed water molecule partially hydrolyzes the highly reactive metal alkoxide. The partially hydrolyzed metal alkoxide reacts with the silicon/metal alkoxide group and leading to the formation of dimeric oxy-alkoxide as shown in Eqs. 15 and 16:

$$\mathrm{H_2O + M(OR'')_x \rightarrow M(OR'')_{x-1}(OH) + R''OH} \qquad (15)$$

$$\mathrm{Si(OR)_{4-x}(R''')_x + M(OR'')_{x-1}(OH) \rightarrow (R''')(OR)_{3-x}Si\text{-}O\text{-}M(OR'')_{x-1} + ROH} \qquad (16)$$

With the help of the CCC method water gradients leading to precipitation of insoluble metal hydroxides can be avoided. However, as shown in Eq. 7 carboxylic acid reacts readily with metal alkoxides result in bidental chelate type of

metal complexes. This complex formation is widely used in order to prevent the precipitation of metal alkoxides during the sol-gel material synthesis [87]. Hence, it might be possible that during the CCC method metal chelates are also formed via the reaction between the carboxylic acid and metal alkoxide. Therefore, instead of controlled water formation, precipitated metal hydroxides are avoided by using less hydrolyzable [87] bidental metal chelates.

In order to increase the thermal expansion coefficient, plasticity (decrease of brittleness) and material adhesion to plastic substrate, several organic network modifiers and/or network formers are incorporated into the sol-gel matrix via non-hydrolyzable Si-C bonds. These functionalities include methyl groups [82], epoxies and methacrylates [12, 85], and isocyanatos with triamines and glycerols [84]. From those organic functionalities, the methyl group has a pure network modifying effect; by substituting one Si-O- bridge by methyl group, the coefficient of thermal expansionis increased from $5 \cdot 10^{-7}$ to about $1 \cdot 10^{-4}$ K^{-1} [17]. Moreover, by reacting polydimethylsiloxane (PDMS) with tetraethoxysilane (TEOS) in a weight ratio of 10:90, the brittleness of the resulting material is reduced from 3.63 (100 % of TEOS) to 1.88 $\mu m^{-½}$ [82]. The index of brittleness is obtained using the ratio H/K_c, where H is the Vickers hardness and K_c is the fracture toughness.

Epoxy, methacrylic and isocyanato triamine/glyserol systems form corresponding polymer types of networks. After material synthesis, polymeric networks can be formed thermally or by UV-assisted polymerization using methacrylic or epoxy functionalities. Methacrylic groups can be polymerized using UV- or thermal radical initiators. In the case of epoxy groups, anionic initiators have to be used during UV-curing. Unfortunately anionic initiators, such as triphenylsulphonium hexafluoro phosphate (Ph_3S)[PF_6], are typically vulnerable to water and therefore polymerization during the material synthesis is preferred. For that purpose, metal alkoxides such as $Zr(OR)_4$ and $Al(OR)_3$ can be used to catalyze the epoxy ring opening during the material synthesis [12, 83]. Isocyanato groups react readily with triamines and glycerols result in organic network formation during the material synthesis [84].

4.1.1.2 Particulate method

In the particulate method, hard coatings are fabricated from functionalized nanoparticles. The most used nanoparticles are TiO_2, ZrO_2 and $AlOOH$ e.g. boehmite [83, 86, 88–89]. In order to avoid Rayleigh scattering, the particle size has to be at least ten times smaller than the wavelength propagating through the material [90]. In particular this means that particle size has to be smaller than 20 nm when operating at visible range.

The functionalizing has been done by reacting nanoparticle suspensions with the silicon alkoxides also used during the polymer method. The most used silanes are 3-glycidyloxypropyl trimethoxysilane (GPMS) and methacryloxypropyl trimethoxysilane (MPTMS). By using the latter silane, UV-curable hard coatings have been achieved by the addition of a suitable radical initiator [86,89]. During the nanoparticle functionalizing, the -OH group on the surface of the nanoparticle reacts with the alkoxide group of the silane. As a result, stable suspensions of nanoparticles coated with GPMS and MPTMS are formed. Before coating suitable modifiers (e.g. dimethacrylates, initiators, and leveling agents) are added to the suspension. After film formation, the coatings are cured using UV- or thermal treatments. In these types of coatings, hard oxide types of nanoparticles are cross-linked together with inorganic and organic networks, resulting in superior abrasion and scratch resistance. A schematic description of the material processing is shown in Figure 16.

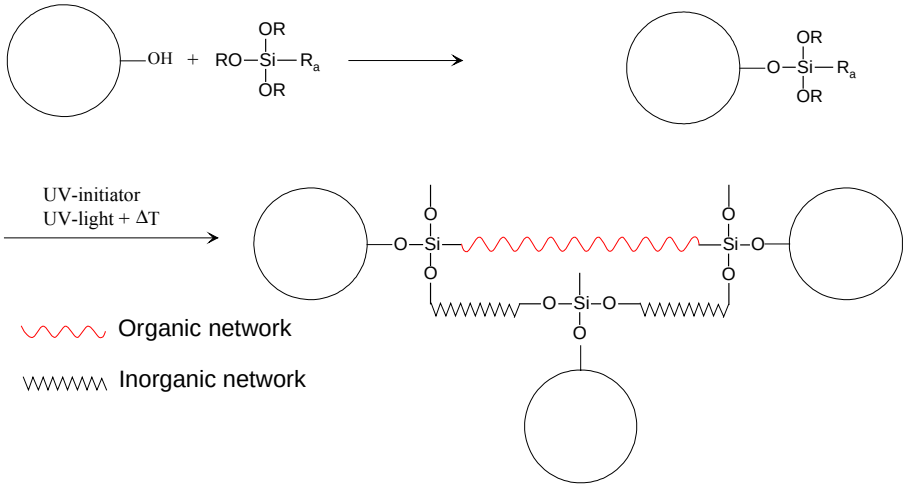

Figure 16. Scheme of the fabrication of particulate hard coating system [85].

4.1.2 NIR-Absorbing molecules

The restrictive factor for the absorption at near-infrared (NIR) wavelengths is the relatively low energy of the NIR-radiation. The energy is too low to excite a simple conjugated double bond system, but too high for absorption through molecular vibration and rotation. Hence, NIR-absorbing molecules have a relatively large size containing long delocalized conjugated double bond systems [91]. Furthermore, NIR-absorption molecules are charged molecules containing an electron acceptor-donor pair and also an inorganic counter ion. The structural

properties of the NIR-absorbing molecules lead to the relatively low solubility of the dye molecules.

Optical excitation in absorption molecules corresponds to the singlet-singlet transition, from which the ground state to first excited state is the strongest [92]. If the energy of the incoming radiation is high enough, transition to higher singlet states occurs. From the application point of view, this is another problem, because the absorption bands of the higher singlet states typically lay at visible wavelengths, reducing the amount of incoming light and disturbing the light vision.

According to the above-mentioned facts, there is a limited number of suitable absorption molecules for military protective eyewear. During our investigations we have chosen the commercially available *N,N,N',N'-tetrakis-(4-dibutylamino-phenyl)-1H,4H-phenylene-1,4-diammonium di-hexafluoro antimonate* (IR165, Figure 17) molecule due to its optical properties [V], solubility in methanol and high molar absorptivity ($2.2 \cdot 10^5$ L mol^{-1} cm^{-1}, in methanol).

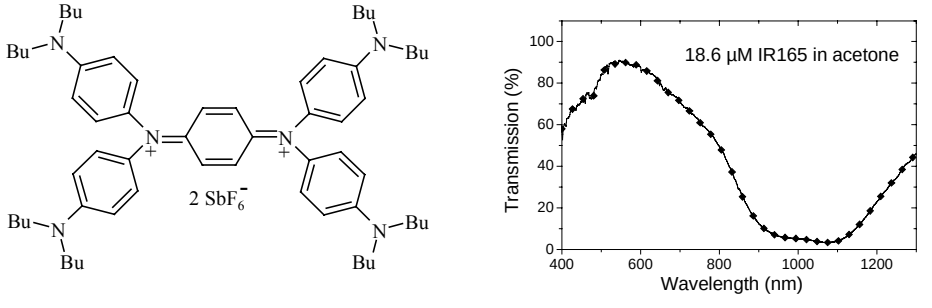

Figure 17. Molecular structure of IR165 and its spectral characteristics in polar solvent [V].

4.1.3 Combined properties

The synthesis of the organic-inorganic hybrid sol-gel materials was related to the earlier studies of H. Schmidt *et al*. [12–13]. Two types of coatings were synthesized in order to investigate the solubility and functionality of the dye molecules in cured films. The precursors for Coating 1 were glysidyloxypropyltrimethoxysilane (GPMS), methacryloxypropyltrimethoxysilane (MPTMS), 2-hydroxyethylmethacrylate (HEMA), tetramethoxysilane (TMOS) and aluminium-tri-sec-butoxide (*Al(O-s-Bu)$_3$*) with molar ratios of 4:1.5:1.5:2:1, respectively. Coating 2 was synthesized from GPMS, propyltrimethoxysilane (PTMOS) and *Al(O-s-Bu)$_3$* with molar ratios of 5:3:2, respectively. PTMOS was

used to decrease the water uptake and the hydrocarbon permeability of the coating [13]. First, the precursor was mixed by vigorous stirring for ten minutes. After this, deionized water soaked in silica gel was added to the solution. Silica gel delivers water to the alkoxide mixture slowly and water gradients may be avoided, preventing the precipitation of the aluminum compounds. The method is comparable with the CCC method.

IR165 was used as the NIR-absorbing dye. IR165 was dissolved in acetone to obtain a 10 mM solution. The final coating solutions were obtained by mixing equal volumes of the sol-gel solution, dye solution and 0.3 wt.-% Byk-306 (leveling agent). The coatings were fabricated by the spray-coating method. After spraying, the films were thermally cured at 80–120°C for 30 minutes. The achieved coating thicknesses were 35 µm and 25 µm for coatings 1 and 2 cured at 80°C, respectively [V].

The organic functionality of the alkoxides in the sol-gel matrix has a drastic effect on the optical characteristics of the dye-doped coatings, Figure 18 [V]. The *Coating with propyl functionality* clearly has insufficient optical properties: (*i*) its optical density is only 2 and (*ii*) the absorption at wavelengths below 500 nm disturbs color-vision remarkably. *Coating with methacrylic functionality* maintains its optical characteristics in hybrid matrix. Optical density of that coating is at the desired level and it does not disturb the color vision [V].

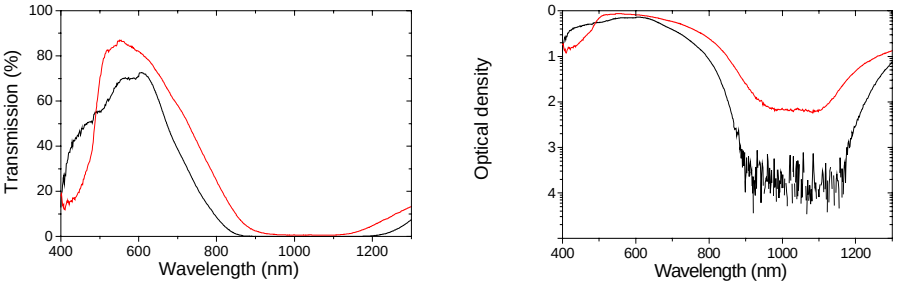

Figure 18. Optical properties of the fabricated coating, cured at 80°C. Black line coating with methacrylic functionality, red line coating with propyl functionality [V].

The tolerance of the coatings against scratching and abrasion were studied according to the ISO 1518 and Taber tests, respectively. Uncoated PC can be scratched with a 100 g load. Coating 1 was scratched when the load was 750 g, whereas Coating 2 required an 800 g load. Polycarbonate was also abraded after a single cycle (CF-10, 500 g) whereas Coating 1 requires 100 cycles and Coating

2 25 cycles. Tests show that the fabricated coatings are clearly more mechanically stable when compared to uncoated polycarbonate substrates.

4.2 Materials for micro-optics: Axicon

The most successful applications for the sol-gel derived multifunctional materials are optical components such as diffractive optical elements (DOE's) [93] and planar channel waveguides [94–95]. Compared to the conventional photoresist-assisted wet lithography, reactive ion etching, electron beam writing, and embossing [96], sol-gel coatings offer a feasible way to produce optical components cost-effectively with precisely controlled properties. The cost efficiency of these components is achieved by introducing organic polymerizable functionalities, in general methacrylics, into the optically transparent matrix. This kind of material simultaneously behaves as an optical core material and UV-photoresist. Typically all directly UV-photopatternable materials fabricated with the sol-gel technique have a negative type of behavior; UV-irradiation leads to reduced solubility of the material. The deposited optical hybrid layer can be patterned to the desired optical structures without the use of an additional photoresist layer leading to a reduced number of process steps and chemicals when compared to conventional photolithographic techniques [93]. Using sol-gel derived materials, optical elements have been also realized with techniques other than UV-fabrication, including laser writing [87], direct electron beam writing (including sub-micron features) [97], and laser holography [98].

Due to the versatility of the sol-gel processing and to the ability to obtain a wide range of different types of materials, the sol-gel technique offers the precise control of crucial optical properties of the materials e.g. transparency at selected wavelengths, refractive indices [87], birefringence [99], and surface roughness [100]. Additionally sol-gel materials can be processed at low temperatures allowing the fabrication of optical elements on the plastics. Furthermore, the fact that inorganic-organic hybrid materials potentially have a higher thermal stability in comparison to plastic elements, results in an enhanced field of applications.

Since *McLeod* introduced and characterized the axicon, which in general is a rotationally symmetric diffractive grating (Figure 19), in 1954, axicons and their generalizations have been under intensive interest and research [101–104]. When an axicon is illuminated (in our case with a collimated Gaussian type of radiation), an axicon diffracts the light with the same radial angle from all areas of the axicon, resulting in a uniform on-axis intensity distribution, more specifically a Bessel beam [101].

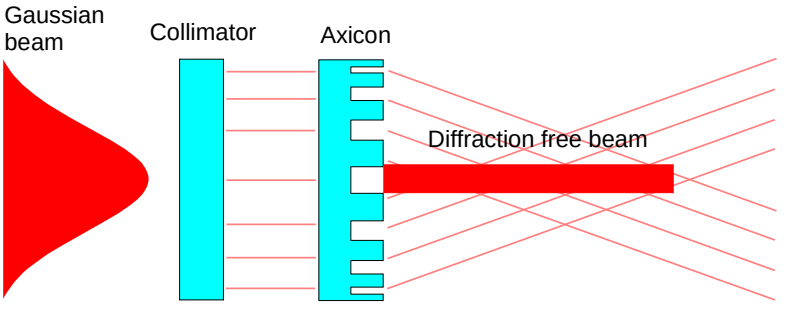

Figure 19. Working principle of the functional axicon element.

4.2.1 Design

During our investigation, axicons for a triangulation measurement device were designed, fabricated and characterized [VI]. In our case, the axicon was designed to perform two functions simultaneously, namely the laser collimation and the actual axicon function. The radial phase profile of the element is obtained from Eq. 17.

$$\phi(r) = -\frac{2\pi}{\lambda}\left[\frac{r^2}{2f} + r\sin(\theta)\right] \tag{17}$$

The parameters used in our design are shown in Table 4 [VI]. For the fabrication, the design of the element was quantized to contain only two-phase levels (binary element). Finally, the phase difference was transformed to the height of the grating lines, h, by using the refractive index, n (1.49 at 850 nm), of the material: $h = \frac{1}{2}\lambda/(n\text{-}1)$.

Table 4. Design parameters of the axicon [VI].

Parameter	Symbol	Value
Wavelength	λ	850 nm
Focal length	f	7.5 mm
Aperture radius	r_{max}	1 mm
Beam length	z_{max}	10mm

The axicon element designed according to the given design parameters (Table 4.) results in features with a maximum line-width of 4.26 µm (central region) and a minimum of 1.82 µm (edge region). Because of this, it was assumed that

lines in the different parts of the fabricated axicons were not produced equally well with all UV-doses used [VI].

The calculated axial intensity profile of the element is shown in Figure 20 [VI]. An 830 nm laser was used in the measurements, which causes some differences between the calculated and measured beams. The oscillations in the intensity profile in Figure 20 are due to diffraction orders higher than ±1 and the sharp aperture edge.

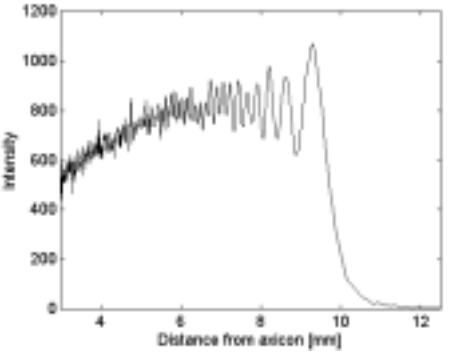

Figure 20. Calculated axial intensity profile produced by the axicon, when it is illuminated by an edge-emitting laser with an elliptical beam profile [VI].

4.2.2 Fabrication and characteristics

The fabrication of the negative tone hybrid material is based on a typical and widely used sol-gel synthesis in which the synthesized methacrylic acid-modified zirconium(IV) isopropoxide complexes are used to increase the refractive index of the metacryloxypropyltrimethoxysilane-derived UV-reactive matrix [87, 93]. Films were made on soda-lime glass substrates by the spin coating method. The spinning speed and time were adjusted to produce approximately 1 μm thick films. After the spinning, axicons were UV-exposed through a "contact" mask. After the UV-exposure, the axicon structures were developed in acetone, i.e. unexposed material was dissolved from the substrate. Finally, the structures were stabilized by annealing them at 160°C for two hours. In Figure 21, the central region of the axicons fabricated using different UV-doses ((a) 250 mJ/cm^2, and (b) 350 mJ/cm^2) are shown [VI]. As expected, there is a clear difference in the line width of the axicons fabricated with different UV-doses.

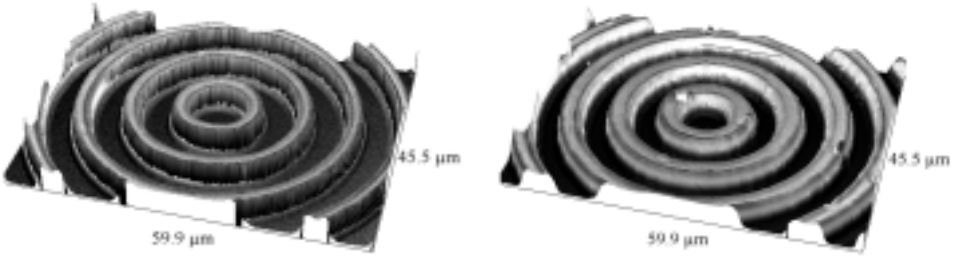

Figure 21. (a) Wyko NT 2000 picture from the central region of the axicon fabricated using a UV-dose of 250 mJ/cm^2. (b) A corresponding picture from the axicon prepared by using a UV-dose of 350 mJ/cm^2 [VI].

The axicon fabricated using a UV-dose of 350 mJ/cm^2 produces the most intense beam (Figure 22). However, there are two main differences between the calculated and measured axial beam profiles [VI]. First, the length of the measured beam is longer than the calculated beam. One reason is that the shorter wavelength used in the measurement increases the beam length by 0.5 mm. In addition, a misfocus of 0.5 mm increases the axial focus by about 1 mm. Therefore we assume that in the measurements both of these effects occurred and produced longer beams than expected from the calculations [VI].

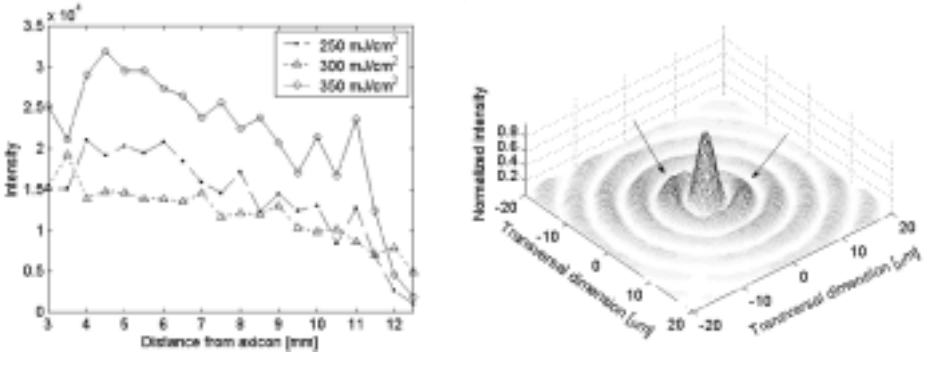

Figure 22. Measured axial intensity profiles of the axicons fabricated with different UV-doses (left). Measured beam profile of the axicon fabricated using an UV-dose of 350 mJ/cm^2 (right) [VI].

Another main difference between the calculated (Figure 20) and measured axial intensity profiles is that the maximum intensity in the calculated profile in-

creases as a function of the distance from the axicon, whereas the maximum intensity in the measured profiles decreases (Figure 22). This is related to the decreased diffraction efficiency at the edge of the element. The shape factor (if compared to the ideal rectangular shape) is assumed and shown to be worse at the edge of the element than in the center [VI]. This is due to the fact that the smaller structures at the edge are not produced as well as the larger structures in the center of the element as noticed during the morphological characterization [VI].

5. Conclusions and outlook

The sol-gel derived hybrid materials offer a feasible way of fabricating multi-functional materials with required functionalities for specific purposes. During this work the synthesis of multifunctional coating materials for three specific applications fields has been presented: *(i)* antimony-doped tin dioxide coatings to be used as transparent anodes, *(ii) a* military laser protective eye-wear coating, suitable for military applications, and *(iii)* a functional micro-optical element, axicon, for triangular measurement devices.

A simplified method of producing conductive and transparent antimony-doped tin dioxide coatings is realized. Argon-plasma treatment of these coatings has been observed to increase the conductivity and decrease the optical transmission of the coatings. Although we have proposed that the changes in electrical and optical properties are related to the oxygen depletion layer and oxygen vacancies, we cannot be sure what causes the observed changes. Further studies are needed in order to understand the effects that occur during the argon-plasma treatment (e.g. HALL-measurements and elemental analysis). Therefore, close attention will be paid to the characterization of the treated and untreated films in the future.

Directly UV-photopatternable tin alkoxide precursors for the fabrication of conductive and transparent thin films were realized using methacrylate and benzoylacetonate functionalities. The obtained conductivity values were around 15 S/cm for single-layered coatings. Conductivities are one order of magnitude lower in comparison to multi-layered coatings fabricated from chlorides without the possibility of direct patterning. Interestingly, in the case of the coatings derived from methacrylic acid modified precursors, conductivity values for UV-irradiated films are higher than for unexposed samples. This is a combined consequence of larger crystal size and more even antimony distribution of the UV-irradiated coatings.

From the application point of view, the sol-gel technique seems to be a relatively inappropriate method for the fabrication of coatings in which bulk material type of properties are required. In order to increase the particle size of the formed crystalline material, novel synthetic routes have to be developed together with film treatment techniques leading to denser materials. One possible solution to larger particle size is the particulate sols in which already crystalline oxide particles are used as precursors. Another possibility is related to our observation that, by using suitable precursors and film treatment techniques, particle size of the material can be increased. Hence, more attention should be paid on the precursor - solution - gel - final material property relationship. This can easily be per-

formed using conventional chemical characterization techniques already introduced during this thesis.

We have successfully incorporated NIR-absorbing dye molecules in mechanically stable coatings. The optical density obtained using a sol-gel matrix with methacrylic functionality is over 4. However, due to the absorbing molecules used, optical density decreases to 2 during some specific environmental tests (US-mil-810D standard) including humidity cycling, water and gasoline immersion (SbF_6^- counter ion), and UVB irradiation. The water stability of the coatings has been already increased using another type of absorbing molecule, but the stability against UVB irradiation is still insufficient.

Sol-gel hybrid-glass materials offer a cost-effective method for the fabrication of micro-optical elements with precisely controlled optical properties on various types of substrates. During this work we have successfully fabricated a diffractive optical element, namely an axicon, whose optical characteristics correspond to design. The material used during the fabrication of the axicon element is not, however, an ideal material for micro-optics fabrication, even though widely used for the micro-optics. The main disadvantage related to this directly photopatternable hybrid glass material is stickiness of the films. Stickiness leads to the fact that the mask used during the patterning cannot be in direct contact with the film. In accordance with this, diffracted light propagates to the unwanted areas, reducing the accuracy of the patterning. Moreover, in order to fabricate a wide range of optical elements, there has to be the capability of fabricating submicron features. New patterning techniques realizing the use of deep UV-irradiation and holographic techniques together with sol-gel derived hybrid-glass materials have to be applied in the future for the preparation of light modulating devices.

According to the results reported in this thesis sol-gel derived multifunctional coating materials are most suitable for use in micro-optics fabrication and in applications realizing different types of functionalities at once. By using these types of materials, the usage of multiple coating during the fabrication of multifunctional materials and optical elements with traditional techniques can be avoided. Military laser-protective eyewear and the axicon element developed during this work are good examples of such materials.

References

1. Brinker, C. J. and Scherer, G. W. Sol-gel Science: The Physics and Chemistry of Sol-Gel Processing. San Diego, CA: Academic Press Inc., 1990. pp. 2–10. ISBN 0-12-134970-5

2. Turner, C. W. Sol-Gel Process-Principles and Applications. Ceramic Bulletin, 1991. Vol. 70, pp. 1487–1490.

3. Bradley, D. C., Mehrotra, R. C., Rothwell, I. P. and Singh, A. Alkoxo and Aryloxo Derivatives of Metals. San Diego, CA: Academic Press Inc., 2001. pp. 3–51. ISBN 0-12-124140-8.

4. Hampden-Smith, M. J., Wark, T. A. and Brinker, C. J. The solid state and solution structures of tin(IV)alkoxide compounds and their use as precursors to form tin oxide ceramics via sol-gel type hydrolysis and condensation. Coordination Chemistry Reviews, 1992. Vol. 112, pp. 81–116.

5. Gamard, A., Jousseaume, B., Toupance, T. and Gampet, G. New Fluorinated Stannic Compounds as Precursors of F-Doped SnO_2 Materials Prepared by the Sol-Gel Route. Inorganic Chemistry, 1999. Vol. 38, pp. 4671–4679.

6. Thomas, I. M. Multicomponent Glasses from the Sol-Gel Process. In: Klein, L. (ed.). Sol-Gel Tecnology for Thin Films, Fibers, Preforms, Electronic and Speciality Shapes. Park Ridge, NJ: Noyes Publications, 1988. pp. 2–16. ISBN 0-8155-1154-X

7. Bradley, D. C., Mehrotra, R. C., Rothwell, I. P. and Singh, A. Alkoxo and Aryloxo Derivatives of Metals. San Diego, CA: Academic Press Inc., 2001. pp. 105–155. ISBN 0-12-124140-8.

8. Hench, L. L. and West, J. K. The Sol-Gel Process. Chemical Reviews, 1990. Vol. 90, pp. 33–72.

9. Brinker, C. J. and Scherer, G. W. Sol-gel Science: The Physics and Chemistry of Sol-Gel Processing. San Diego CA: Academic Press Inc, 1990. Pp. 22–42. ISBN 0-12-134970-5

10. Livage, J., Sanchez, C., Hendry, M. and Doeuff, S. The chemistry of the sol-gel process. Solid State Ionics, 1989. Vol. 32/33, pp. 633–638.

11. Brinker, C. J. and Scherer, G. W. Sol-gel Science: The Physics and Chemistry of Sol-Gel Processing. San Diego CA: Academic Press Inc., 1990. pp. 357–402. ISBN 0-12-134970-5.

12. Schmidt, H. and Seiferling, B. Chemistry and applications of inorganic-organic polymers (organically modified silicates). In: Cheetham, A. K., Brinker, C. J. and Mecartney, M. L. (eds.). Better Ceramics Through Chemistry II. Palo Alto, CA, USA, 1986. Pittsburgh PA: Materials Research Society, 1986. pp. 739–750. (Materials Research Society Symposia Proceedings, Vol. 73.) ISBN 0-931837-39-1

13. Schmidt, H. and Wolter, H. Organically modified ceramics and their applications. Journal of Non-Crystalline Solids, 1990. Vol. 121, pp. 428–435.

14. Schmidt, H. Organically modified ceramics-materials with "history" or "future". In: Uhlmann, D. R. and Ulrich, D. R. (eds.). Ultrastructure Processing of Advanced Materials. New York NY: John Wiley & Sons Inc., 1992. pp. 409–423. ISBN 0-471-52986-9

15. Chandler, C. D., Fallon, G. D., Koplick, A. J. and West, B. O. The Structures of Mono and Bis β-diketonate Tin(IV) Alkoxide Complexes. Australian Journal of Chemistry, 1987. Vol. 40, pp. 1427–1439.

16. Verdenelli, M., Parola, S., Hubert-Pfalzgraf, L. G. and Lecocq, S. Tin dioxide thin films from Sn(IV) modified alkoxides – synthesis and structural characterization of $Sn(OEt)_2(\eta^2\text{-acac})_2$ and $Sn_4(\mu_3\text{-O})_2(\mu_2\text{-OEt})_4(OEt)_6(\eta^2\text{-acac})_2$. Polyhedron, 2000. Vol. 19, pp. 2069–2075.

17. Schmidt, H. Organically modified silicates by the sol-gel process. In: Brinker, C. J., Clark, D. E. and Ulrich, D. R. Better Ceramics Through Chemistry. Elsevier Science, 1984. pp. 327–335. (Materials Research Society Symposia Proceedings, Vol. 32.) ASIN 0444008985

18. Stevens, M. P. Polymer Chemistry: An Introduction. 2nd Edition. New York, NY: Oxford University Press, 1990. p. 16. ISBN 0-19-505759

19. Tadanaga, K., Katata, N. and Minami, T. Super-Water-Repellent Al_2O_3 Coating Films with High Transparency. Journal of American Ceramic Society, 1997. Vol. 80, pp. 1040–1042.

20. Kololuoma, T. Nissilä, S. M. and Rantala, J. T. Synthesis of transparent conductive polycerams. In: Dunn, B. S., Pope, E. J. A., Schmidt, H. K. and Yamane, M. (eds.). Sol-Gel Optics V. San Jose, CA, USA, 26–28 January, 2000. Bellingham, WA, USA: Society of Photo-Optical Instrumentation

Engineers, 2000. pp. 218–225. (Proceedings of SPIE, Vol. 3943.) ISBN 0-8194-3560-0

21. Gordon, R. G. Criteria for Choosing Transparent Conductors. MRS Bulletin, 2000. Vol. 25, pp. 52–57.

22. Park, S.-S. and Mackenzie, J. D. Sol-gel-derived tin oxide thin films. Thin Solid Films, 1995. Vol. 258, pp. 268–273, and references therein.

23. Chopra, K. L., Major, S. and Pandya, D. K. Transparent Conductors-a Status Review. Thin Solid Films, 1983. Vol. 102, pp. 1–46.

24. Lambert, C. M. Heat mirror coatings for energy conserving windows. Solar Energy Materials, 1981. Vol. 6, pp. 1–41.

25. Kohl, D. Surface processe in the detection of reducing gases with SnO_2-based devices. Sensors and Actuators, 1989. Vol. 18, pp. 71–113.

26. Shanthi, E., Banerjee, A., Dutta, V. and Chopra, K. L. Annealing characteristics of tin oxide films prepared by spray pyrolysis. Thin Solid Films, 1980. Vol. 71, pp. 237–244.

27. Park, S.-S. and Mackenzie, J. D. Thickness and microstructure effects on alcohol sensing of tin oxide thin films. Thin Solid Films, 1996. Vol. 274, pp. 154–159.

28. Senguttuvan, T. D. and Malhotra, L. K. Sol gel deposition of pure and antimony doped tin dioxide thin films by non alkoxide precursors. Thin Solid Films 1996. Vol. 289, pp. 22–28.

29. Ray, S. C., Karanjai, M. K. and DasGupta, D. Tin dioxide based transparent semiconducting films deposited by the dip-coating technique. Surface and Coatings Technology, 1998. Vol. 102, pp. 73–80.

30. Cachet, H., Gamard, A., Campet, G., Jousseaume, B. and Toupance, T. Tin dioxide thin films prepared from new alkoxyfluorotin complex including covalent Sn-F bond. Thin Solid Films, 2001. Vol. 388, pp. 41–49.

31. Stjerna, B., Olsson, E. and Granqvist, C. G. Optical and electrical properties of radio frequency sputtered tin oxide films doped with oxygen vacancies, F, Sb, or Mo. Journal of Applied Physics, 1994. Vol. 76, pp. 3797–3817.

32. Maddalena, A., Dal Maschio, R., Dire, S. and Raccanelli, A. Electrical conductivity of tin oxide films prepared by the sol-gel method. Journal of Non-Crystalline Solids, 1990. Vol. 121, pp. 365–369.

33. Mulla, I. S., Soni, H. S., Rao, V. J. and Sinha, A. P. B. Deposition of improved optically selective conductive tin oxide films by spray pyrolysis. Journal of Materials Science, 1986. Vol. 21, pp. 1280–1288.

34. Shanthi, E., Dutta, V., Banerjee, A. and Chopra, K. L. Electrical and optical properties of undoped and antimony-doped tin oxide films. Journal of Applied Physics, 1980. Vol. 51, pp. 6243–6251.

35. Bellingham, J. R., Phillips, W. A. and Adkins, C. J. Instrinc performance limits in transparent conducting oxides. Journal of Material Science Letter, 1992. Vol. 11, pp. 263–265.

36. Bisht, H., Eun, H.-T., Mehrtens, A. and Aegerter, M. A. Comparison of spray pyrolyzed FTO, ATO and ITO coatings for flat and bent glass substrates. Thin Solid Film, 1999. Vol. 351, pp. 109–114.

37. Cao, X., Cao, L., Yao, W. and Ye, X. Influences of dopants on the electronic structure of SnO_2 thin films. Thin Solid Films, 1998. Vol. 317, pp. 443–445.

38. Viirola, H. and Niinistö, L. Controlled growth of antimony-doped tin dioxide thin films by atomic layer epitaxy. Thin Solid Films, 1994. Vol. 251, p. 127.

39. Demiryont, H., Nietering, K. E., Surowiec, R., Brown, F. I. and Platts, D. R. Optical properties of spray-deposited tin oxide films. Applied Optics, 1987. Vol. 26, pp. 3803–3810.

40. Haitjema, H. and Elich, J. Physical properties of fluorine-doped tin dioxide films and the influence of ageing and impurity effects. Solar Energy Materials, 1986. Vol. 16, pp. 79–90.

41. Takahashi, Y. and Wada, Y. Dip-Coating of Sb-doped SnO2 Films by Ethanolamine-Alkoxide Method. Journal of Electrochemical Society, 1990. Vol. 137, pp. 267–272.

42. Aegerter, M. A., Reich, A., Ganz, D., Gasparro, G., Pütz, J. and Krajewski, T. Comparative study of SnO_2:Sb transparent conducting films produced by various coating and heat treatment techniques. Journal of Non-Crystalline Solids, 1997. Vol. 218, pp. 123–128.

43. Goebbert, C., Nonninger, R., Aegerter, M. A. and Schimdt H. Wet chemical deposition of ATO and ITO coatings using crystalline nanoparticles redispersable in solutions.Thin Solid Films, 1999. Vol. 351, pp. 79–84.

44. Chatelon, J. P., Terrier, C., Bernstein, E., Berjoan, R. and Roger, J. A. Morphology of SnO_2 thin films obtained by the sol-gel process. Thin Solid Films, 1994. Vol. 247, pp. 162–168.

45. Senguttuvan, T. D. and Mahlhotra, L. K. Electronic structure of sol-gel derived SnO_2 thin films. Journal of Physics and Chemistry of Solids, 1997. Vol. 289, pp. 19–24.

46. Kololuoma, T., Rantala, J. T., Vähäkangas, J. and Laitinen, R. S. Transparent conductive sol-gel thin films for photonic applications. In: Righini, G. C. and Najafi, S. (eds.). Integrated Optics Devices III. San Jose, CA, USA, 25–27 January, 1999. Bellingham, WA, USA: Society of Photo-Optical Instrumentation Engineers, 2000. pp. 134–142. (Proceedings of SPIE, Vol. 3620.) ISBN 0-8194-3090-0

47. Hiratsuka, R. S., Pulcinelli, S. H. and Santilli, C. V. Formation of SnO_2 gels from dispersed sols in aqueous colloidal solutions. Journal of Non-Crystalline Solids, 1990. Vol. 121, pp. 76–83.

48. Orel, B., Lavrenčič-Štangar, U., Crnjak-Orel, Z., Bukovec, P. and Kosec, M. Structural and FTIR spectroscopic studies of gel-xerogel-oxide transitions of SnO_2 and SnO_2:Sb powders and dip-coated films prepared via inorganic sol-gel route. Journal of Non-Crystalline Solids, 1994. Vol. 167, pp. 272–288.

49. Tsunashima, A., Yoshimizu, H., Kodaira, K., Shimada, S. and Matsushita, T. Preparation and properties of antimony-doped SnO_2 films by thermal decomposition of tin 2-ethylhexanoate. Journal of Materials Science, 1986. Vol. 21, pp. 2731–2734.

50. Olivi, P., Pereira, E. L., Varella, J. A. and Bulhões, L. O. de S. Preparation and Characterization of Dip-Coated SnO_2 Film for Transparent Electrodes for Transmissive Electrochromic Devices. Journal of Electrochemical Society, 1993. Vol. 140, pp. L81–L82.

51. Giuntini, J. C., Granier, W., Zanchetta, J. V. and Taha, A. Sol-gel preparation and transport properties of a tin oxide. Journal of Materials Science Letters, 1990. Vol. 9, pp. 1383–1388.

52. Racheva, T. M. and Critchlow, G. W. SnO_2 thin films prepared by the sol-ge process. Thin Solid Films, 1997. Vol. 292, pp. 299–302.

53. Terrier, C., Chatelon, J. P., Berjoan, R. and Roger, J. A. Sb-doped SnO2 transparent conducting oxide from the sol-gel dip-coating technique. Thin Solid Films, 1995. Vol. 263, pp. 37–41.

54. Gonzales-Olivier, C. J. R. and Kato, I. Sn(Sb)–oxide sol-gel coatings on glass. Journal of Non-Crystalline Solids, 1986. Vol. 82, pp. 400–410.

55. Lee, S.-C., Lee, J.-H., Oh, T.-S. and Kim, Y. H. Fabrication of tin oxide film by sol-gel method for photovoltaic solar cell system. Solar Energy Materials & Solar Cells, 2003. Vol. 75, pp. 481–487.

56. Cobiannu, C., Savaniu, C., Buiu, O., Dascalu, D., Zaharescu, M., Parlog, C., van der Berg, A. and Pesz, B. Tin dioxide sol-gel derived thin films deposited on porous silicon. Sensors and Actuators B, 1997. Vol. 43, pp. 114–120.

57. Puetz, J., Chavelt, F. N. and Aegerter, M. A. Transparent conducting coatings on glass tubes. In: Pope, E. J. A, Schmidt, H. K., Dunn, B. S. and Shibata, S. (eds.). Sol-Gel Optics VI. Seattle, WA, USA, 10–11 July, 2002. Bellingham, WA, USA: Society of Photo-Optical Instrumentation Engineers, 2002. pp. 73–80. (Proceedings of SPIE, Vol. 4804.) ISBN 0-8194-4572-X

58. Dislich, H. Thin films from the sol-gel process. In: Klein, L. (ed.). Sol-Gel Tecnology for Thin Films, Fibers, Preforms, Electronic and Speciality Shapes. Park Ridge, NJ: Noyes Publications, 1988. pp. 50–79. ISBN 0-8155-1154-X

59. Gasparro, G., Pütz, J., Gantz, D. and Aegerter, M. A. Parameters affecting the electrical conductivity of SnO_2:Sb sol-gel coatings. Solar Energy Materials & Solar Cells, 1998. Vol. 54, pp. 287–296.

60. Canut, B., Teodorescu, V., Roger, J. A., Blanchin, M. G., Daoudi, K. and Snadu, C. Radiation-induced densification of sol-gel SnO_2:Sb films. Nuclear Instruments and Methods in Physics Research B, 2002. Vol. 191, pp. 783–788.

61. Terrier, C., Chatelon, J. P., Roger, J. A., Berjoan, R. and Dubois, C. Analysis of Antimony Doping in Tin Oxide Thin Films Obtained by the Sol-Gel Method. Journal of Sol-Gel Science and Technology, 1997. Vol. 10, pp. 75–81.

62. Nakanishi, Y., Suzuki, Y., Nakamura, T., Hatanaka, Y., Fukuda, Y. Fujisawa, A. and Shimaoka, G. Coloration of Sn-Sb-O thin films. Applied Surface Science, 1991. Vol. 48–49, pp. 55–58.

63. Kololuoma, T. and Rantala, J. T. Unpublished results.

64. Tamai, T., Ichinose, N., Kawanishi, S., Nishii, M., Sasuga, T., Hashida, I. and Mizuno, K. Patterning of SnO_2 Thin Films by Combination of Lithographic Photoirradiation and Pyrolysis of an Organotin polymer. Chemistry of Materials, 1997. Vol. 9, pp. 2674–2675.

65. Tadanaga, K., Owan, T., Morinaga, J., Urbanek, S. and Minami, T. Fine Patterning of Transparent Conductive SnO_2 Thin Films by UV-irradiation. Journal of Sol-Gel Science and Technology, 2000. Vol. 19, pp. 791–794.

66. Cui, B. J., Wang, A., Edleman, N. L., Ni, J., Lee, P., Armstrong, N. R. and Marks, T. J. Indium Tin Oxide Alternatives-High Work Function Transparent Conducting Oxides as Anodes for Organic Light-Emitting Diodes. Advanced Materials, 2001. Vol. 13, pp. 1476–1480.

67. Kikuta, K., Suzumori, K., Takagi, K. and Hirano, S. Patterning of Tin Oxide Film from Photoreactive Precursor Solutions Prepared via the Addition of N-Phenydiethanolamine. Journal of American Ceramic Society, 1999. Vol. 82, pp. 2263–2265.

68. Wei, Q., Zheng, H. and Huang, Y. Direct patterning ITO transparent conductive coatings. Solar Energy Materials & Solar Cells, 2001. Vol. 68, pp. 383–390.

69. Lin-Vien, D., Cothuo, N. B., Fateley, W. G. and Graselli, J. G. The Handbook of Infrared and Raman Characteristic Frequencies of Organic Molecule. London: Academic Press Inc., 1991. pp. 141. ISBN: 0-12-451160-0

70. Kololuoma, T., Tolonen, A., Johansson, L.-S., Campbell, J. M., Lärkkäinen, A. H. O., Halttunen, M., Haatainen, T. and Rantala, J. T. Fabrication and characterization of Sb-doped SnO_2 thin films derived from methacrylic acid-modified tin(IV)alkoxides. In: Pope, E. J. A, Schmidt, H. K., Dunn, B. S. and Shibata, S. (eds.). Sol-Gel Optics VI. Seattle, WA, USA, 10–11 July, 2002. Bellingham, WA, USA: Society of Photo-Optical Instrumentation Engineers, 2002. pp. 106–114. (Proceedings of SPIE, Vol. 4804.) ISBN 0-8194-4572-X

71. Kololuoma, T. *et al.* To be submitted.

72. Barnum, D. W. Electronic absorption spectra of acetylacetonato complexes-I. Journal of Inorganic Nuclear Chemistry, 1961. Vol. 21, pp. 221–237.

73. Zhao, G. and Tohge, N. Preparation of photosensitive gel films and fine patterning of amorphous Al_2O_3-SiO_2 thin films. Materials Research Bulletin, 1998. Vol. 33, pp. 21–30.

74. Zhao, G., Tohge, N. and Nishii, J. Fabrication and Characterization of Diffraction Gratings Using Photosensitive Al_2O_3 Gel Films. Japanese Journal of Applied Physics, part 1, 1998. Vol. 37, pp. 1842–1846.

75. Shinmou, K., Tohge, N. and Minami, T. Fine-Patterning of ZrO_2Thin Films by the Photolysis of Chemically modified Gel Films. Japanese Journal of Applied Physics, part 2, 1994. Vol. 33, pp. L1181–L1184.

76. Tohge, N., Zhao, G. and Chiba, F. Photosensitive gel films prepared by the chemical modification and their applicatio to surface relief gratings. Thin Solid Films, 1999. Vol. 351, pp. 85–90.

77. Kololuoma, T., Maaninen, A., Tolonen, A. and Rantala, J. T. To be submitted.

78. Smilowitz, L., McBranch, D., Klimov, V., Grigorova, M., Robinson, J. M. B., Weyer, J., Koskelo, A., Mattes, B. R., Wang, H. and Fudl, F. Fullerene Doped Glasses as Solid State Optical Limiters. Synthetic Metals, 1997. Vol. 84, pp. 931–932.

79. Lund, D. J., Edsalland P. and Masso, J. D. Another look at saturable absorbers for laser eye protection. In: Bryan, P. K. and Sliney, D. H. (eds.). Laser Safety, Eye Safe Laser Systems, and Laser Eye Protection. Los Angeles, CA, USA, 16–17 January, 1990. Bellingham, WA, USA: Society of Photo-Optical Instrumentation Engineers, 1990. pp. 193–201. (Proceedings of SPIE, Vol. 121.) ISBN 0-8194-0248-6

80. Hofacker, S. and Schottner, G. Hybrid pigments via sol-gel processing. Journal of Sol-Gel Science and Technology, 1998. Vol. 13, pp. 479–484.

81. Dubois, A., Canva, M., Brun, A., Chaput, F. and Boilot, J.-P. Enhanced photostability of dye molecules trapped in solid xerogel matrices. Synthetic Metals, 1996. Vol. 81, pp. 305–308.

82. MacKenzie, J. D., Huang, Q. and Iwamoto, T. Mechanical Properties of Ormosils. Journal of Sol-Gel Science and Technology, 1996. Vol. 7, pp. 151–161.

83. Kasemann, R., Schmidt, H. and Wintrich, E. A New type of a sol-gel-derived inorganic-organic nanocomposite. In: Cheetham, A. K., Brinker, C. J., Mecartney, M. L. and Sanchez C. Better Ceramics Through Chemistry VI. San Francisco, CA, USA, 4–8 April, 19941. Pittsburgh PA: Materials Research Society, 1994. pp. 915–921. (Proceedings of the 1994 MRS Spring Meeting, Vol. 346.) ISBN 1-55899-069-0

84. Wen, J. and Wilkes, G. L. Synthesis and Characterization of Abrasion Resistant Coating Materials Prepared by the Sol-Gel Approach: I. Coatings Based on Functionalized Aliphatic Diols and Diethylenertiamine. Journal of Inorganic and Organometallic Polymers, 1995. Vol. 5, pp. 343–375.

85. Gilberts, J., Tinnemans, A. H. A., Hogerheide, M. P. and Koster, T. P. M. UV Curable Hard Transparent Hybrid Coating Materials on Polycarbonate Prepared by the Sol-Gel Method. Journal of Sol-Gel Science and Technology, 1998. Vol. 11, pp. 153–159.

86. Schmidt, H. K., Oliveira, P. W. and Sepeur, S. Novel ormocers and nanomers for coatings. In: Vincenzini, P. (ed.). Ceramics: Getting into the 2000's – Part C. Florence, Italy, 14–19 June, 1998. Faenca, Italy: Techna Srl, 1999. pp. 451–465. (Proceedings of the CIMTEC-World Ceramics Congress and Forum of New Materials, Advances in Science and Technology 15.) ISBN 88-86538-16-2

87. Schmidt, H., Krug, H., Kasemann, R. and Tiefensee, F. Development of optical waveguides by sol-gel techniques for laser printing. In: Bray, P and Kreidl, N. J. (eds.). Submolecular Glass Chemistry and Physics. Boston, MA, USA, 3–4 September, 1991. Bellingham, WA, USA: Society of Photo-Optical Instrumentation Engineers, 1991. pp. 36–43. (Proceedings of SPIE, Vol. 1590.) ISBN 0-8194-0721-6

88. Mennig, M., Oliveira, P. W. and Schmidt, H. Interference coatings on glass based on photopolymerizable nanomer material. Thin Solid Films, 1999. Vol. 351, pp. 99–102.

89. Sepeur, S., Kunze, N., Werner, B. and Schmidt, H. UV curable hard coatings on plastics. Thin Solid Films, 1999. Vol. 351, pp. 216–219.

90. Kaino, T. Polymer Optical Fibers. In: Hornak, L. A. (ed.). Polymers for Lightwave and Integrated Optics: Technology and Applications. New York: Marcel Dekker, 1992. pp. 1–24. ISBN 0-82-478697-1

91. Fabian, J., Nakazumi, H. and Matsuoka, M. Near-Infrared Absorbing Dyes. Chemical Reviews, 1992. Vol. 92, pp. 1197–1226.

92. Brackmann, U. In Lambdachrome Laser Dyes. Göttingen, Germany: Lambda Physik GmbH, 1997.

93. Rantala, J. T., Äyräs, P., Levy, R., Honkanen, S., Descour, M. R. and Peyghambarian, N. Binary-phase zone-plate arrays based on hybrid sol-gel glass. Optics Letters, 1998. Vol. 23, pp. 1939–1941, and references therein.

94. Fardad, M. A., and Fallahi, M. Organic-Inorganic Materials for Integrated Optoelectronics. Electronic Letters, 1998. Vol. 34, pp. 1940–1941.

95. Coudray, P., Chisham, J., Malek-Tabrizi, A., Li, C.-Y., Andrews, M. P., Peyghambarian, N. and Najafi, S. I. Ultraviolet light imprinted sol-gel silica glass waveguide devices on silicon. Optics Communications, 1996. Vol. 128, pp. 19–22.

96. Baraldi, L., Kunz, R. E. and Meissner, J. High-precision molding of integrated optical structures. In: Gallagher, N. C. and Roychoudhuri, C. Miniature and Micro-Optics and Micromechanics. San Diego, CA, USA, 14–15 July, 1993. Bellingham, WA, USA: Society of Photo-Optical Instrumentation Engineers, 1993. pp. 21–31. (Proceedings of SPIE, Vol. 1992.) ISBN 8194-1241-4

97. Rantala, J. T., Nordman, N., Nordman, O., Vähäkangas, J., Honkanen S. and Peyghambarian, N. Sol-gel hybrid glass diffractive elements by direct electron-beam exposure. Electronics Letters, 1998. Vol. 34, pp. 455–456.

98. Courday, P., Moreau, Y., Etienne, P. and Porgue, J. New developments in integrated optics using the Sol-gel process. In: Andrews, M. P and Najafi, I. S. Sol-Gel and Polymer Photonic Devices. Proceedings of SPIE, 1997. Vol. CR68. pp. 286–303.

99. Toyoda, S., Ooba, N., Hikita, M., Kurihara T. and Imamura, S. Propagation loss and birefringence properties around 1.55 μm of polymeric optical waveguides fabricated with cross-linked silicone. Thin Solid Films, 2000. Vol. 370, pp. 311–314.

100. Kärkkäinen, A. H. O, Tamkin, J. M., Rogers, J. D., Neal, D. R., Hormi, O., Jabbour, G. E., Rantala, J. T. and Descour, M. R. Direct photolithographic deforming of organomodified siloxane films for micro-optics fabrication. Applied Optics, 2002. Vol. 41, pp. 3988–3998.

101. Popov, S. Y., Friberg, A. T., Honkanen, M., Lautanen, J., Turunen, J. and Schnabel, B. Apodized annular-aperture diffractive axicons fabricated by continuous-path-control electron beam lithography. Optics Communications, 1998. Vol. 154, pp. 359–367.

102. Popov, S. Y. and Friberg, A. T. Design of diffractive axicons for partially coherent light. Optics Letters, 1998. Vol. 23, pp. 1639–1641.

103. Honkanen, M. and Turunen, J. Tandem systems for efficient generation of uniform-axial-intensity Bessel fields. Optics Communications, 1998. Vol. 154, pp. 368–375.

104. Artl, J. and Dhoklia, K. Generation of high-order Bessel beams by use of an axicon. Optics Communications, 2000. Vol. 177, pp. 297–301.

Appendices of this publication are not included in the PDF version. Please order the printed version to get the complete publication (http://www.vtt.fi/inf/pdf/)

Published by

Series title, number and report code of publication

VTT Publications 499
VTT–PUBS–499

Author(s)
Terho Kololuoma

Title

Preparation of multifunctional coating materials and their applications

Abstract

Sol-gel technique has been utilized for the fabrication of multifunctional inorganic organic hybrid materials for specific applications. Synthesized methacrylic acid and benzoylacetone modified tin alkoxide precursors were used for the first time for the realization of directly UV-photopatternable antimony-doped tin dioxide coatings. These single-layered coatings have transmission values over 80 % at visible wavelengths and maximum electrical conductivity values around 15 S/cm. In comparison, multi-layered coatings without UV-photopatternability properties were fabricated. In this case, electrical conductivities are in the range of 10^2 S/cm. A novel material technique approach for laser protective eyewear was utilized for the synthesis and preparation of the mechanically tolerant and near-infrared absorbing filter coatings. Optical densities from 2 to 4 at laser threat wavelength, a ten fold increase in scratch resistance, and a hundred-fold increase in abrasion resistance, compared to uncoated polycarbonate substrates, were obtained by using absorbing dye-molecule doped sol-gel materials. Fabrication of a diffractive optical element, namely axicon, using hybrid-glass materials was demonstrated for the first time. Hybrid-glass material was tailored to fulfill the requirements of the functional axicon element.

Keywords
sol-gel materials, antimony-doped tin dioxide, micro-optical elements, protective coatings

Activity unit
VTT Electronics, Optoelectronics, Kaitoväylä 1, P.O.Box 1100, Fin–90571 OULU, Finland

ISBN			Project number
951–38–6227–5 (soft back ed.) 951–38–6228–3 (URL:http://www.vtt.fi/inf/pdf/)			E3SU00093
Date	Language	Pages	Price
July 2003	English	62 p. + app. 33 p.	
Name of project		Commissioned by The Tauno Tönning Foundation	
Series title and ISSN VTT Publications 1235–0621 (soft back ed.) 1455–0849 (URL: http://www.vtt.fi/inf/pdf/)		Sold by VTT Information Service P.O.Box 2000, FIN–02044 VTT, Finland Phone internat. +358 9 456 4404 Fax +358 9 456 4374	

Sol-gel technique has been utilized for the fabrication of multifunctional inorganic organic hybrid materials for specific applications. Synthesized methacrylic acid and benzoylacetone modified tin alkoxide precursors were used for the first time for the realization of directly UV-photopatternable antimony-doped tin dioxide coatings. These single-layered coatings have transmission values over 80 % at visible wavelengths and maximum electrical conductivity values around 15 S/cm. In comparison, multi-layered coatings without UV-photopatternability properties were fabricated. In this case, electrical conductivities are in the range of 10^2 S/cm. A novel material technique approach for laser protective eyewear was utilized for the synthesis and preparation of the mechanically tolerant and near-infrared absorbing filter coatings. Optical densities from 2 to 4 at laser threat wavelength, a ten fold increase in scratch resistance, and a hundred-fold increase in abrasion resistance compared to uncoated polycarbonate substrates, were obtained by using absorbing dye-molecule doped sol-gel materials. Fabrication of a diffractive optical element, namely axicon, using hybrid-glass materials was demonstrated for the first time. Hybrid-glass material was tailored to fulfill the requirements of the functional axicon element.

Tätä julkaisua myy
VTT TIETOPALVELU
PL 2000
02044 VTT
Puh. (09) 456 4404
Faksi (09) 456 4374

Denna publikation säljs av
VTT INFORMATIONSTJÄNST
PB 2000
02044 VTT
Tel. (09) 456 4404
Fax (09) 456 4374

This publication is available from
VTT INFORMATION SERVICE
P.O.Box 2000
FIN–02044 VTT, Finland
Phone internat. +358 9 456 4404
Fax +358 9 456 4374

ISBN 951–38–6227–5 (soft back ed.)
ISSN 1235–0621 (soft back ed.)

ISBN 951–38–6228–3 (URL: http://www.vtt.fi/inf/pdf/)
ISSN 1455–0849 (URL: http://www.vtt.fi/inf/pdf/)